AGING BEHAVIOUR OF INCONEL 718 PPREPARED BY LASER PROCESSING

A DISSERTATION

Submitted in partialfulfilment of the

requirements for the award of the degree

of

MASTER OF TECHNOLOGY

in

METALLURGICAL AND MATERIALS ENGINEERING

by

AJAY SINGH TOMAR

DEPARTMENT OF METALLURGICAL AND MATERIALS ENGINEERING

INDIAN INSTITUTE OF TECHNOLOGY ROORKEE

ROORKEE – 247667, INDIA

MAY, 2016

INDIAN INSTITUTE OF TECHNOLOGY ROORKEE

CANDIDATE'S DECLARATION

I hereby certify that the work which is being presented in the thesis, entitled **"AGING BEHAVIOUR OF INCONEL 718 PREPARED BY LASER PROCESSING "**has submitted by "**Mr. AJAY SINGH TOMAR**" in partial fulfillment of the requirements for the degree of **Master of Technology** in the **Department of Metallurgical and Materials Engineering with specialization** in **"Industrial Metallurgy"**, Indian Institute of Technology Roorkee, is an authentic record of my own work carried out during the period from May,2015 to April, 2016 under the supervision of **Dr. Sadhan Ghosh**, **Assistant Professor,** Department of Metallurgical and Materials Engineering, Indian Institute of Technology Roorkee, Roorkee.

The matter embodied in the thesis has not been submitted to any of the University/Institute for the award of any other degree.

Date:

Place: (Ajay Singh Tomar)

CERTIFICATE

This is to certify that the above statement made by the candidate is correct to the best of our knowledge.

(Dr. Sadhan Ghosh)
Assistant Professor
Department of Metallurgical & Materials Engineering
Indian Institute of Technology Roorkee
Roorkee-247667

ACKNOWLEDGEMENT

I take immense pleasure in thanking **Department of Material Science and Metallurgy, Indian Institute of Technology** for giving me nice and peaceful environment carry out this project work.

I am highly obliged to **Dr. Sadhan Ghosh, Assistant Professor, Department of Metallurgical and Materials Engineering, Indian Institute of Technology Roorkee,** for encouraging me to undertake this dissertation as well as providing me all the necessary guidance and motivation throughout this dissertation work. He has displayed unique tolerance and understanding at every step of progress. It is my proud privilege to have carried out this dissertation work under his valuable guidance.

I wish to express my sincere thanks to **Dr. S.K. Nath**, Professor and Ex- HOD) and **Dr. Anjan Sil** , Head of the Department, Metallurgical and Materials Engineering Department, Indian Institute of Technology Roorkee, for his help to carry out this dissertation.

Special thanks to technical staff of Metallographic lab, Material Testing lab, Fabrication lab and others for their valuable support, guidance and co-operations to carry out this dissertation.

I would like to acknowledge all friends for their valuable information share, and developing love and confidence in me throughout the work.

My deepest gratitude goes to my parents for their unbound love and immeasurable moral and emotional support who have buffered the blow that I have received from the system time to time. Any words of gratefulness will be insufficient for their concern in my wellbeing. Finally, I owe everything to the almighty to shower his blessing so that my effort could reach the destination.

IIT Roorkee
Date: (Ajay Singh Tomar)

ABSTRACT

The inconel 718 is a commercially successful nickel-base superalloy widely used in nuclear reactors, heavy machinery and other high-temperature applications because of its good corrosion resistance, mechanical properties and structural stability up to 650°C. for high temperature application directionally solidified or single crystal is used because of its better creep resistance and thermo-mechanical fatigue behavior in the absence of grain boundaries. But the manufacturing cost of single crystal is more this is one of the major problems. Hence, there developed interest in finding an alternative route synthesizing inconel 718 by laser deposition on mild steel substrate. An intense laser heating of the powder feed followed by cooling of the metal powders (via substrate) leads to a dendritic microstructure in layer wise growth of the material: this subsequently gets exposed to further heating during multilayer growth of the material up to 28 mm in length and 15 mm in thickness.

As it is known, precipitation of inter-metallic phases during heat treatment improves creep resistance in inconel 718. Prior to this, a solutionizing treatment is also necessary at 955°C for 1 hr. Thus, a microstructure comparison of the as-prepared sample was done with respect to the samples heat treated at 718°C for 8h (HT2) and another at 718°C for 8h+ 621°C for 18 h (HT1), as commercial practice.

CONTENTS

LIST OF FIGURES

LIST OF TABLES

LIST OF ABBREVIATIONS

FCC	Face centered cubic
HCP	Hexagonal closed packed
BCT	Body center tetragonal
TCP	Topological Closed Packed
ODS	Oxide dispersion strengthened
CAD	Computer-aided design
CAM	Computer-aided manufacturing
DMD	Direct metal deposition
DS	Directional solidification
Fig.	FIGURE
SEM	Scanning electron microscope
SRO	Short range ordering
LRO	Long range ordering
HT1	Heat treatment of sample 1
HT2	Heat treatment of sample 2
RT	Room temperature
XRD	X-ray diffraction
IN718	INCONEL 718

CHAPTER 1 INTRODUCTION

1.1 Introduction

Superalloys, as the name implies have characteristics that make them different from other materials. Modern superalloys consist multiple elements, may be more than 14 elements. This makes them different entity from the past alloys which can be dominated by one element. If we look our past we can realize that materials have a dominant impression on our civilizations. These materials have a direct or indirect effect on the culture, tradition, and daily life. Inconel 718, nickel-base superalloy, was developed by International Nickel Corporation in the 1950s and found many applications in turbine and aero engine components. Nickel-based superalloys have lot of development during over the last four decades. Inconel 718, a Ni-Cr-Fe superalloy, has been used in many applications such as gas turbine blades, aero engine, nuclear reactors due to its excellent properties as corrosion resistance, creep resistance and oxidation resistance, thermal fatigue, also easiness of forging, welding and brazing, are the advantages of Inconel 718. Inconel 718 can retain its mechanical properties in a range of temperature due to solid-solution strengthening and precipitation strengthening. Nevertheless, its high hardness and low thermal conductivity characteristics make it difficult to apply conventional machining methods because of tool over-wear and poor work-piece surface integrity [1] [3].

According to, high temperature materials should possess the following characteristics:-

I. Ability to withstand loading at an operating temperature close to its melting point.
II. A substantial resistance to mechanical degradation over extended period of time.
III. Tolerance of sever operating environments.

These high temperature materials commonly called superalloys are developed to face the challenges of efficient energy demands but at the same time minimizing greenhouse gas emissions.

1.2 Types of superalloys

There are various superalloys developed by several industries, which have different application in aero industry, power generation and nuclear power plants etc. They are available in cast (usually heat treated or otherwise processed) or wrought (often heat treated or otherwise processed) forms. The chemical composition of each of them varies, based on the desired characteristics. The current superalloys are usually consists of 10 to 15 elements. But there are three main categories that are jointly called superalloys as mentioned below. They possess high level of temperature insensitivity or stability and are widely used as base materials for high temperature applications.

1. Nickel base superalloy
2. Iron-nickel superalloy
3. Cobalt base superalloys

Inconel 718 superalloy is a family of austenitic nickel-chromium base superalloy. These alloys are generally used at temperature above 450 °C, as at these temperatures ordinary steel and titanium alloys are losing their strengths; also corrosion is common in steels at this temperature.

1. **Nickel based superalloys:** The solid solution γ phase constitutes the Ni phase, which has a Face Centered Cubic (FCC) crystal structure [1]. Usually used when high strength is the required, for the temperature range of 1024º to 1371 °C. They are a widely used and renowned group of austenitic alloys. The unique characteristic of this group of superalloys are their application without compromising their integrity close to their melting temperatures. Ni-base superalloys can be divided into three types:
   - **a.** Solid solution strengthened alloys: which usually contains the following alloying elements; Fe, Co, Cr, Mo, W, Ti, Nb and Al. Such as Haynes230 and HasteloyX. Among these Al, Cr, W and Mo are potential solid–solution strengtheners because of different atomic radius as compared to Ni [2]. They are more suitable for processing, for example weldability [3] and can also be manufactured into complex geometries from powders using laser melting techniques as described in [4].
   - **b.** Precipitation (age) hardened alloys: usually contain Al, Ti, Ta and sometimes Nb that facilitate the formation of γ′ and γ′′ precipitates in the γ matrix. Such as

Inconel 718, 738, 939 and Wasp alloy. it is evident that precipitation hardened alloys possess higher strengths compared to solid solution strengthened alloys and are widely used in high temperature applications.

c. Oxide dispersion strengthened (ODS) alloys: alloys contain fine oxide particles of Y_2O_3 about 0.5 to 1%.

2. **Nickel-iron superalloys:** The most important class of this group are those alloys that are strengthened by an intermetallic compound precipitation in an FCC matrix. The common precipitate is γ′ [5]. Alloys such as Inconel 718, which has γ′ and γ″ precipitates are classed as iron-nickel base because of their higher percentage of Fe, but are considered to be nickel based. Others superalloys in this group consist of stainless steel strengthened by solid-solution hardening. They are primarily used as a wrought material and are comparatively cheaper than Ni base alloys.
3. **Cobalt based superalloy:** are strengthened by the combination of carbides and solid solution hardeners. Cobalt crystallizes in the Hexagonal closed packed (HCP) crystal structure below 417°C, as shown in the figure 1. They possess excellent corrosion resistance at high temperatures (980-1100 °C) because of their higher chromium contents. They possess better weldability and thermal fatigue resistance as compared to nickel based alloy. But cobalt-base alloys are more likely to precipitate undesirable sigma (σ) and Topological Closed Packed (TCP) phases. Depending on the application / composition involved it may be wrought or cast.

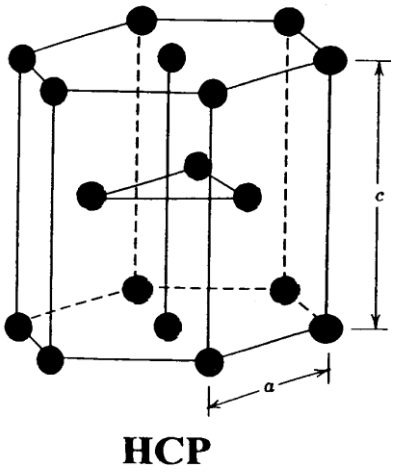

Figure 1: HCP structure of cobalt

1.3 Physical metallurgy of nickel and its alloys

Nickel is the fifth rarest element on earth and has a Face Centered Cubic (FCC) crystal structure as shown in figure 2. It belongs to the family of transition metals and exists in the form of five stable isotopes. Transition elements are often called transition metals (possess the properties of metals) or d-block elements, includes group 3-12 in the periodic table. The elements that are alloyed with Ni to form superalloys and the phases they contribute to also is mentioned in the figure 2.

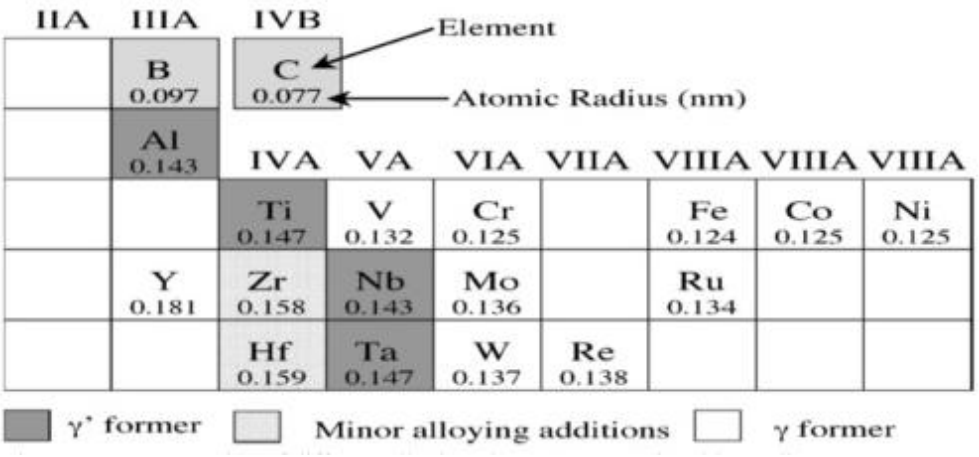

Figure 2: Elements added in Ni to form superalloys

The melting temperature is ~ 1455 °C and has a density of 8907 kg/m^3 at room temperature. The characteristic that give nickel excellent mechanical properties even at high temperature is its negligible yield strength / temperature sensitivity. Another reason is that the FCC crystal structure that is both tough (toughness is the measure of resistance to fracture which is measured in units of energy) and ductile because of the cohesive energy arising from the bonding provided by the outer electrons. Secondly, Ni is stable in its austenitic form temperature to its melting point (i-e no phase transformation). Also low diffusion rate in FCC metals give good micro-structural stability even at very high temperatures [5].

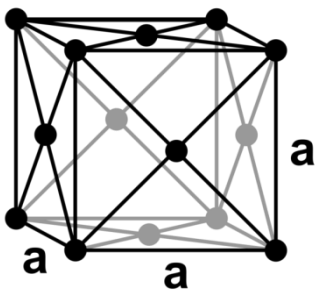

Figure 3: FCC structure of Ni

Ni based superalloys belongs to the family of austenitic nickel- chromium based superalloys that typically contains 80% Ni and 20% Cr. Several alloying elements are included in different percentages depending on the need to achieve better mechanical properties. Ni- based alloys are usually strengthened by precipitation (age) hardeners, they may be wrought or cast depending on the application / composition involved.

The modern complex superalloy composition is due to unique phase chemistry and structure. The microstructure consists of different phases. The important ones such as gamma phase (γ), gamma prime (γ′), gamma double prime (γ″), delta phase (δ) and various carbides and borides are explained below.

- The gamma phase (γ): The gamma phase is the matrix phase of nickel-based superalloys in which the other phases reside. It exhibits a FCC crystal structure and its composition mainly consist of Ni with other elements such as Co, Cr, Mo, Ru, Re, and Fe [5].
- Gamma prime (γ′): forms the precipitate phase, which is usually coherent with the γ-matrix and is the main strengthening precipitate in nickel based superalloys. Similar to the γ phase γ′ have an ordered FCC crystal structure. γ′ mainly consist of Ni, Al, Ti, and Ta i-e Ni3(Al,Ti) [5].
- Gamma double prime (γ″): is a strong coherent metastable precipitate with a body center tetragonal (BCT) structure, it is the primary strengthening precipitate. The γ″ unit cell precipitate i.e. Ni_3Nb consists of Ni and Nb is shown in figure 3 [1], is usually found in Ni-Fe superalloys. At higher temperature γ″ become unstable and can transform into δ phase [6].

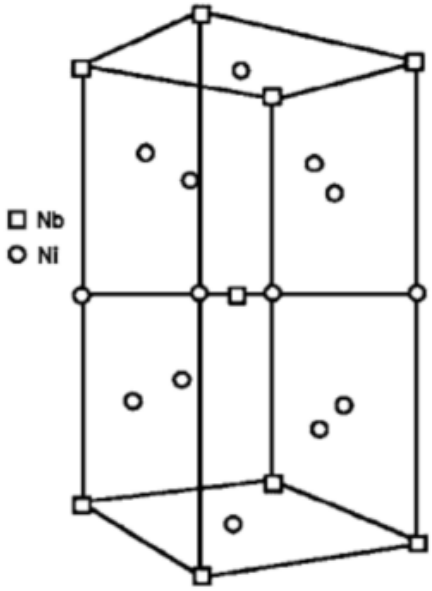

Figure 4**:** BCT structure of gamma double prime (γ″)

- Delta phase (δ): is a non-hardening precipitate usually present at grain boundaries. The loss of hardening is due to depletion of γ″. The structure is orthorhombic and the δ phase improves the creep rupture and grain boundary sliding resistance. It is composed mainly of Ni, Nb and Ti.
- Carbides and borides: Carbide usually forms when carbon reacts with Ti, Ta and Hf and result in MC carbides. Where M represents elements such as Cr, Mo, Ti, Ta, or Hf. The MC carbides break-down during service to other species, such as M23C6, M6C, M7C3, and M3B2. These decomposed compounds usually reside in the γ grain boundaries [5]. Borides are found in superalloy in the form of M3B2, having a tetragonal unit cell, Which is also present in grain boundaries and improve the creep rupture resistance of superalloys [3].

Other phases: For example TCP, μ, σ, and laves etc. are present in the form of plates and needles. Under some conditions these can result in lower rupture strength and increase the creep rupture strength [35]. Although it is not desirable to have these compounds.

CHAPTER 2 LITERATURE REVIEW

2.1 LASER PROCESSING

Laser processing is also termed as laser metal deposition, selective laser melting or direct metal deposition, which can produce three-dimensional parts by using CAD/CAM software. These techniques are being used in various industries for manufacturing, repair, layer by layer net like structures. The main advantages of laser metal deposition are lead time and minimization of waste material. Plasma welding is having high deposition rate than laser metal deposition, but it can produce better coating, with less distortion with sound surface finish. So laser technique is used for costly material parts. [11] [13].

Laser metal deposition is a new arising laser manufacturing technology that added laser manufacturing with quick models making and form a solid freeform fabrication process. Laser metal deposition has the ability to control the temperature of the melted pool, dimensional accuracy and composition of the deposit metal. This process has been developed in many industries and laboratories by the different names such as laser powder melting technique or laser net shaping technique, but the basic principles is same in all the technologies. A high-power laser beam is used to create a melt pool of the powder which is delivered by the tiny holes to create metal pool on the substrate metal. A computer numerical control system or computer-aided design system is used to control the laser beam motion and the path of the tool according to the three-dimensional object we want to create, laser beam create the component layer by layer[16] [18].

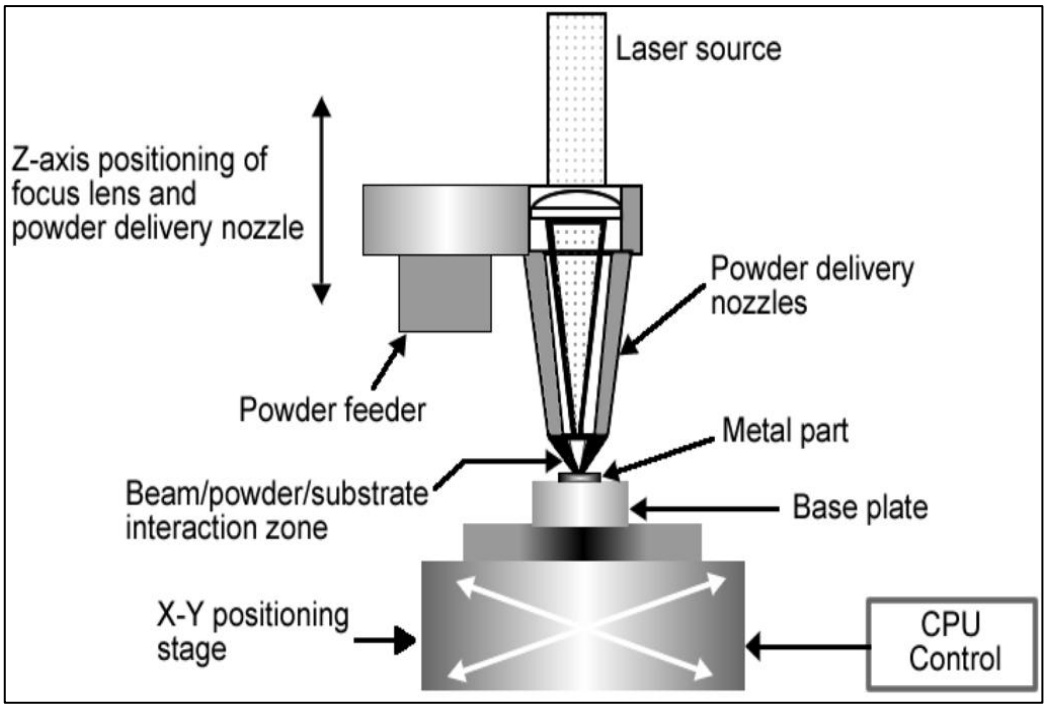

Figure 5: Schematic diagram of laser processing

Direct metal deposition (DMD), due to its importance to create a dense part, flexibility in feed rate and shape precision, has been accepted as a promising manufacturing technique. By laser metal deposition, the geometrically complex shape and high dimensional accuracy can be achieved without doing any subsequent process which is not possible in conventional methods. The required microstructures of direct metal deposition (DMD) processed parts are definitely affected by the physical and chemical reaction occurs in melt pool and these reactions lead to non-equilibrium process of laser technique. So there is lot of research efforts are required to optimize the laser parameters to get desired microstructure and mechanical properties of fabricated components [11] [12].

2.2 DEVELOPMENT OF INCONEL 718 BY LASER PROCESSING

A laser metal deposition system which was developed in University of Michigan used to create two types of sample A and B, with different laser scanning patterns uni-axial and bi-axial which schematically shown in fig.6 [11]. A 6 kW CO_2 laser with a spot size of 0.5 mm used in this experiment INCONEL 718 powder was used in this experiment and the mesh sizes of the powder particles was -100 to +325. The powder had a composition of 53.5 Ni, 19 Cr, 18 Fe, 5 Nb, 3 Mo, 1 Ti and 0.5 Al in weight%. Laser deposition parameters (laser power: 750 watts, scanning speed: 6.25 mm/s; powder feed rate: 0.2 g/s) was kept constant for both deposits. To prevent the melt pool from oxidation, helium was used as a shielding, as well as a powder carrier gas. Two 50 mm long and 3.2 mm high deposits were made by successive deposition of 16 layers on a polycrystalline Inconel 718 rolled plate of dimensions 100 mm ×30 mm ×15 mm. The laser deposition direction of all layers was same (left to right) in deposit A. While, a forward and backward deposition pattern was used to create deposit B. In this deposition pattern laser scan is altered by 180° from the previous layer [11] [16].

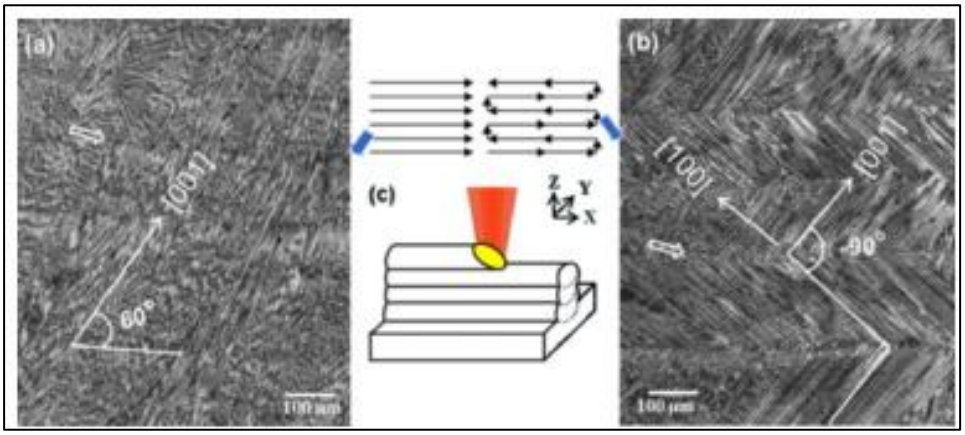

Figure 6: Optical micrographs of the as-deposited IN718 samples produced with two different laser beam scanning patterns

The primary dendrites growing direction are at an angle of 60º from the substrate. In deposit B, as we can see in Figure 6b ordered columnar dendrites are present in the longitudinal cross section. The growth direction of primary dendrites changing in each layer by 90º with respect to the primary dendrites growth direction, the growth direction of primary dendrites is altered by +45º and -45º, corresponding to adjacent layers,

respectively. Note that, even though for the both deposits A and B the laser metal deposition parameters were constant, after that change in the laser beam scanning pattern from unidirectional to bidirectional (backward and forward) changes the dendrite growth direction from 60º to 45º. In direct metal deposition, the previously deposited layer or substrate work as a heat sink and heat flow in the one direction only. During solidification, primary dendrites always grow in the opposite direction to the heat flow direction, which is perpendicular to the solid–liquid interface. Since the local heat flow is always unidirectional and perpendicular to the solidification front. So dendrites grow perpendicular to the solid-liquid front and form a columnar dendritic structure locally. However, solidification of a material in the form of columnar dendrites does not always make a single crystal structure. In columnar dendrites, the crystal growth is one axis orientation almost all dendrites, while other two axis remain free to grow. Hence, columnar dendrites can make single grain or poly grain depending on the other two axes of the dendrites. Columnar dendrite leads to a single crystal only when all three crystal axes of a dendrite are parallel to the corresponding Crystal axes of all other dendrites in the sample.

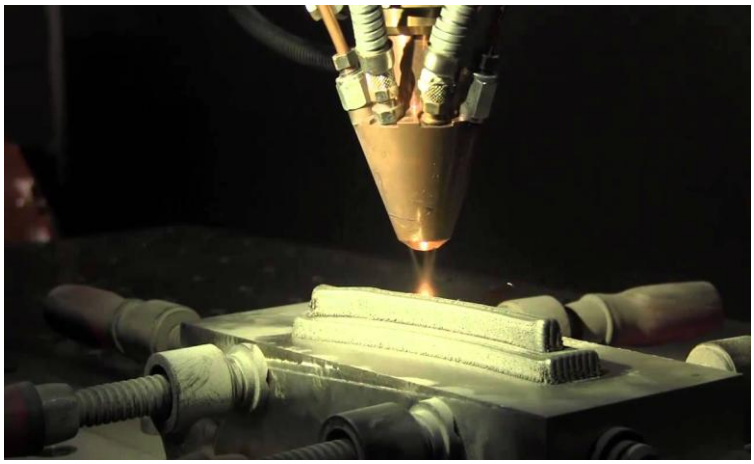

Figure 7: Metal deposition process in which metal is deposited over the substrate

To understand the concept of single crystallinity and polycrystallinity of a deposited metal by laser metal deposition, showing the cross-sections view of deposits A and B, respectively in figure 6. The optical image of deposit A and B shows the dendrites orientation angle 60º in deposit A and 45º in deposit B. it has been seen that the morphology of the grain growth in deposit A is different from deposit B. In deposit A, most of the grains are aligned in same direction and the number of grains in deposit A is

also higher than the deposit B. So we understand by this, bidirectional laser processing develops less grains compared to the unidirectional laser processing. So due to change in 90º growth direction the layers shows a zig-zag shaped pattern[14] [17] [23].

In FCC, [100] directions is having fastest rate of solidification. In general, solidification occurs due to the nucleation and growth of crystals. Solidification depends upon the conditions, either nucleation or grain growth any can be predominant. For example, if laser metal deposition is doing on a single crystalline substrate, which is oriented in such a way that any one of the [100] directions of that substrate remain parallel to the local heat flow direction, and then solidification will occur only in the form of epitaxial growth from the substrate. Consequently, a single-crystalline structure is maintained from the substrate to the clad. However, when laser cladding is conducted on a polycrystalline substrate, only those grains of the substrate grow that have a [100] crystallographic direction that is parallel to the local heat flow direction [11] [21].

In the case of bidirectional laser metal deposition, the nucleation and growth mechanism is same as in the first layer of deposit A, as mentioned above. From the second layer, due to the change in the laser scan pattern, there is a different process of nucleation and grain growth. In this experiment, primary dendrites grew at an angle of about 60º to the substrate in the first layer. Due to the backward and forward laser beam scan pattern in deposit B, the growth direction of the primary dendrites is expected to change by +60º and -60º in the adjacent layers, respectively. However, optical micrograph (Fig. 6b) shows that the dendrite growth angle was +45º and -45º in the second layers onwards. This 15º change in dendrite growth direction is the consequence of the preferred growth direction of FCC crystal in the [100] directions. During solidification of FCC metals and alloys, secondary dendrites grow perpendicular to the primary dendrites as the [100] directions are perpendicular to each other. To change the dendrite growth direction by 60º in subsequent layers, the nucleation of new grains is required at the layer boundaries. However, to change the primary dendrite growth direction by 90º, no nucleation is required because the secondary dendrites of the previous layer can serve as a growth front for the primary dendrites of new layer. In solidification, the driving force (free energy) required for nucleation is much more than that required for grain growth. Hence, in deposit B, the primary dendrite growth direction is altered by 15º from the heat flow direction to maintain the right-angle relationship between the primary dendrite growth direction of subsequent layers necessary to avoid a nucleation barrier. Hence,

solidification occurs mostly by the epitaxial growth of primary dendrites from the secondary dendrites of previous layers in deposit B. This epitaxial growth occurs from those grains which have a [100] direction oriented at an angle of about 45º to the layer interface, and the growth of the other grains ceases. As a result, the number of grains is decreased and the grains become larger at the upper part of the clad.

2.3 DIRECTIONAL SOLIDIFICATION (DS)

The directional solidification of superalloys was introduced after the sixties. In the directional solidification, the solidification direction and the grain boundaries are aligned parallel to each other. This alignment corresponds with the axis of the principal stress of that component. After the directional solidification the final structure consist of dendrite grains in [001] direction or the direction of the load [21].

Stresses at higher temperature have a dominant effect on the grain boundaries which is perpendicular to the stress direction. So, by aligning these grain boundaries can minimize the site of failures and the stresses on the superalloys can be reduced.

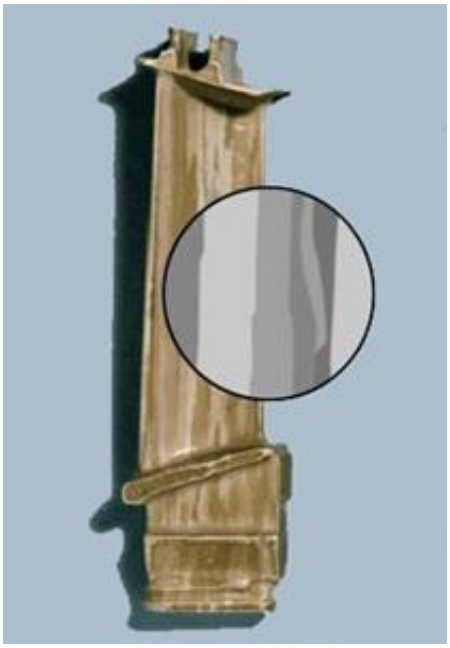

Figure 8: Directionally solidified turbine blade

Directionally solidified components have the creep resistance between the single crystal and the equiaxed grains. Directionally solidified turbine blades increase the thermal fatigue five times than the conventionally prepared turbine blades due to the orientation of grain boundaries at [001] direction of the applied stress [26].

2.4 ADVANTAGE OF LASER PROCESSING

Laser metal deposition is used in various applications, preparation of three dimensional components and repair applications.

- LMD reduces the waste material during manufacturing
- LMD reduces the cost of tooling which is higher in conventional methods
- LMD is used for parts repair which are costly to repair or very difficult to repair precisely
- It reduces the lead time of component
- Customization of parts on the fly
- LMD is used for deposition of novel metals
- Repair of mould tool surfaces
- LMD is used for making original part, hybrid manufacturing
- LMD provide easiness to the deposition of the reactive metals, without the use of protective atmosphere
- Used for depositions of various materials such as Nickel base superalloy, titanium superalloy(Ti-6Al-V4) and also high strength steels
- Powder recycling methods for better process efficiency
- Deposition of metallic glasses and amorphous materials.
- LMD provides small voids or porosity, highly dense component can be produce
- Small heat affected zone
- LMD also provide high solidification rate

The one of the best advantage of laser metal deposition is the ability to metal deposition for existing component for repair. Laser metal deposition also gives the facility for near net shape manufacturing which reduces waste material and tooling costs.

2.5 STRENGTHENING MECHANISMS

Strengthening of superalloys is essential for the purpose of obtaining the desirable high-temperature properties. It can be obtained through either solid-solution strengthening or precipitation hardening.

Creep resistance is an example of interaction between different hardening mechanisms. In early stages of the creep solid-solution strengthening is largest contributor effect on the creep resistance. The solid-solution effect decreases with time whereas the contribution of the precipitation hardening increases.

2.5.1 Solid solution strengthening

It is heating of an alloy to an appropriate temperature, holding it at that temperature long enough to cause one or more constituents to enter into a solid solution and then cooling it rapidly enough to hold these constituents in solution. Subsequent precipitation heat treatments allow controlled release of these constituents either naturally (at room temperature) or artificially (at higher temperatures).

Most solution heat treatments often soften or anneal. And the alloys that are strengthened by SHT are called solution strengthened alloy. Elements in solid solution usually increase yield and tensile strength, other possibilities to increase strength is having finer grains.

Solid solution is best described as a homogeneous crystalline structure in which one or more types of atoms or molecules may be partly substituted for the original atoms or molecules without changing the structure. This substitution has a strengthening effect on the material. Common strengthening elements are chromium, cobalt, iron, molybdenum, rhenium, tantalum and tungsten [7]. As already mentioned in chapter 1.3, solid-solution strengthening takes place in γ phase. The addition of for example molybdenum expands the lattice and cobalt reduces the lattice when replacing iron in the superalloy matrix. An expansion of the lattice creates an internal strain. The expansion affects the mismatch with the strengthening precipitate phase. It has been shown that the stacking fault energy is reduced in the presence of solid-solution strengtheners. This will make it more difficult for dislocations, thus cross-slip at high temperatures is restrained [8] [9].

Solid solution strengtheners can also have a beneficial influence on the corrosion and oxidation resistance. Superalloys with sufficiently large chromium content will form a protective oxide film that covers the surface [8].

2.5.2 Precipitation strengthening

They are done in order to bring out the desirable strengthening precipitates and control other secondary phases. They include carbides, borides, TCP etc. The aging process increases hardness and strength but at the cost of reduction in ductility. As described in

chapter 1.3, gamma prime is formed during aging by the precipitation of aluminium and titanium. The slightly different lattice parameter of γ' creates a small misfit important for two reasons. First of all it guarantees a low γ/γ' surface energy which is essential for a stable microstructure and improves the properties at elevated temperatures. Secondly, a negative misfit, i.e. γ' has a smaller lattice parameter than γ, will facilitate the formation of rafts and by those means possibly reduce the creep rate. The misfit is controlled by the composition of the superalloy, particularly by altering the aluminium-titanium ratio, but also by the aging temperature [8] [10].

2.6 MECHANISM OF AGING

The strength of metals is improved by restrict the motion of dislocations through the metals. One approach to achieving this improvement is to form a uniform distribution of closely spaced sub-micron sized particles throughout an alloy. The particles, which restrict the dislocation motions in the alloy are known as precipitate. Not every alloy can be precipitation strengthened. The particles are formed by precipitation, which involves a series of heat treatment steps. The first step is solution heat treatment. This involves heating the alloy up to a temperature that results in the atoms of the alloying element being dissolved within the solid structure formed by the array of atoms of the main element. For Al-Cu alloys, the copper atoms dissolve into the array of aluminum atoms. The dissolved structure is then retained at ambient temperatures by cooling the alloy rapidly, such as by water quenching.

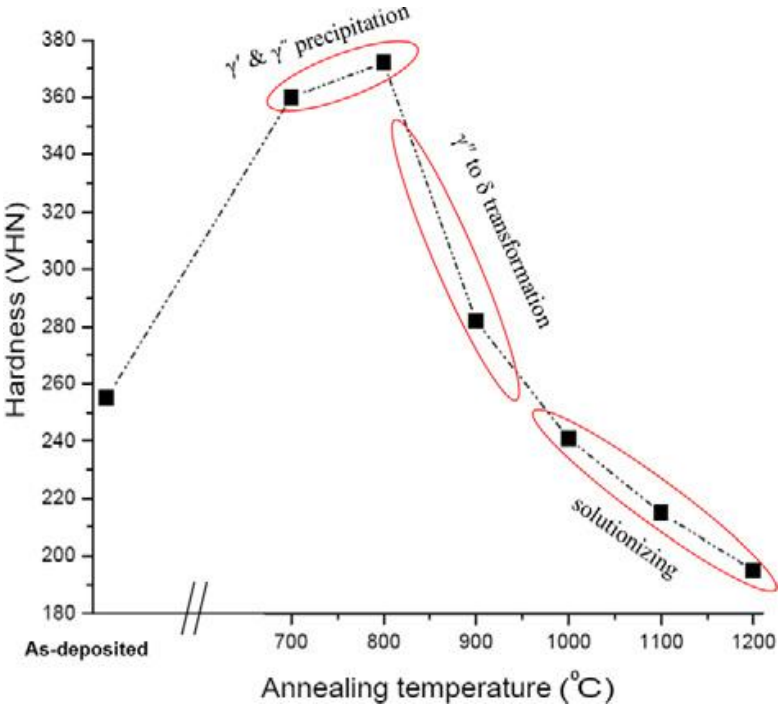

Figure. 9: Variation in hardness with aging temperature of laser deposited IN718

After cooling, precipitates are formed either by natural aging or artificial aging. With natural aging, the precipitates form at room temperature. With artificial aging, the precipitates form when an alloy is heated to a temperature lower than the solution heat treatment temperature. Only certain alloys will undergo natural aging. The other alloys must be artificially aged.

Regardless of the aging process, as the precipitation process proceeds the precipitates go through a series of stages, with changes in the size, form and composition of the precipitates. The particular stage of the precipitates has a direct influence on the strength of the alloy. For artificially aged alloys, this is controlled by the aging temperature and time. At any particular aging temperature, there is an aging time at which the alloy will reach its maximum strength. This maximum strength corresponds to a specific stage of the form and composition of the precipitates. Aging for a time that is too short or too long will result in less than maximum alloy strength. For artificially aged alloys, the aging temperature affects the maximum strength that can be obtained, and the time required to reach maximum strength. For naturally aged alloys, the strength increases over time. The time required to reach maximum strength depends on the alloy. Finally, precipitation strengthening can be combined with cold-working to give even greater alloy strength.

2.7 AGING EFFECT IN SUPERALLOYS

2.7.1 Contraction in superalloys

Shrinkage during use of superalloys and the fundamental mechanisms have been discussed in several studies [26] [27]. Marucco [27] measured lattice contraction after aging at intermediate temperatures between 450°C 600°C in 20Cr-25Ni steel, Sanicro 71 and Inconel 690 which amounted to 0.024, 0.040 and 0.038 % respectively. This study also show that due to the aging there arose of a little ordered area in the alloys. Nath et al. have been involved in several studies [27], to find out the aging effects on different nickel-based alloys, such as Nimonic 80A, a wrought nickel-based precipitation-hardened superalloy used as a bolting material in steam turbines. By use of X-ray diffractometry they proved that the lattice parameter was reduced due to aging at 450-600°C and the kinetics of the contraction was investigated. The maximum lattice parameter contraction was obtained during aging at 450°C for 30000 h and measured 0.115 %. According to Nath et al. the lattice contraction was due to short range ordering (SRO) and long range ordering (LRO) arisen during aging. Electron diffraction studies performed on Nimonic 80A corroborated the existence of SRO based on Ni_2Cr and the transformation into LRO owing to long-term aging.

The lattice parameter contraction depends on the composition of the ordered phase. Marucco and Nath [27] have measured the lattice parameter contraction in Ni_2Cr and Ni_3Cr after aging at 475°C. Ni_3Cr exhibited a small contraction in the neighbourhood of 0.05 % after 10 000 h. The lattice parameter contraction in Ni_2Cr under the same conditions are almost 5 times larger.

In previous work carried out at by Nath, the lattice contraction in different nickel-based superalloys and the austenitic stainless steel X6CrNiTi18-10 was measured. Cylindrical specimens of the length 100 mm were aged at 450, 500 and 550°C and the shrinkage strain was measured after 300, 1000 and 3000 hours in a coordinate measurement machine.

They found that, it is obvious that the contraction of the alloys is significant already after 300 h of aging and between 300 h and 1000 h the shrinkage rate is slowing down and is almost constant between 1000 h and 3000 h. The lattice parameter of the alloys was measured before and after the aging with X-ray diffraction.

2.7.2 Short range ordering (SRO) and long range ordering (LRO)

Short range ordering arises in all Ni-Cr alloys, irrespective of the presence of other alloy elements. Small, ordered areas in the size of nanometers are formed in an otherwise disordered matrix. The ordering takes place when atoms of different types are more attracted to each other than the same type. The short range ordered phase forms at stoichiometric compositions, e.g. AB, A_2B and A_3B or at off-stoichiometric compositions also but there is a condition of lower kinetics. Ni_2Cr is a orthorhombic ordering phase that occurs commonly in Ni superalloys. The SRO formation takes place during either cooling from solid-solution temperature or at lower aging temperature. The degree of SRO decreases with temperature, but it is also affected by the composition. Studies on ternary Ni-Cr-Fe alloys have shown that the enhancement of Ni content increases the degree of SRO and the shortage of Fe content has the opposite effect [26] [27].

Long time aging below a critical temperature T_c will, for certain alloy compositions, result in growth of SRO nuclei, changes short range ordering phase into long term ordering phase. T_c depends on the composition of the alloy, but is normally located between 530°C and 580°C [27].

Even if long range ordered is non-existing above T_c but short range ordered can exist at temperatures above T_c in stoichiometric alloys A_xB_y alloys which would be long range ordered at lower temperatures, See Figure 10 for example

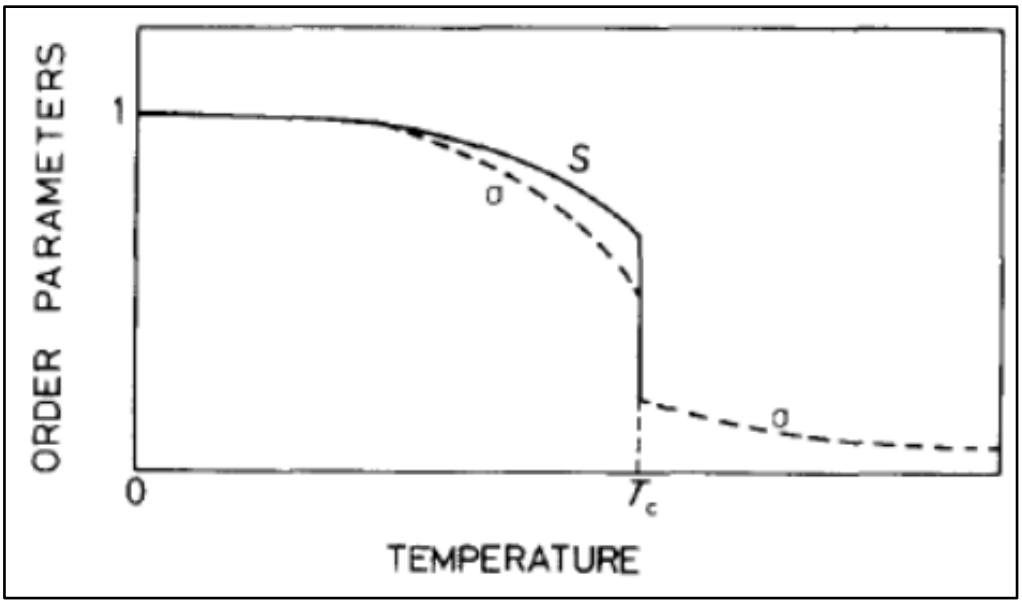

Figure 10 SRO represents by σ and LRO represents by S

According to Rtishchev [28] SRO and LRO are formed if chromium content of 25-35 at% in binary Ni-Cr superalloy. In commercial superalloys, the formation of LRO is possible only when chromium content in γ phase after the γ' precipitation have to exceed 25%.

The tendency of Ni-Cr based superalloys to form LRO can be described by the Z-criterion [28]. Z is calculated on the atom content in γ, after precipitation of γ' and minor phases, according to Equation 1:

$$Z = \frac{Ni}{Cr+W+Mo} \qquad \text{..... Equation 1.}$$

According to Rtishchev, LRO occurs at approximate value of Z<3.0. The Ni_2Cr superlattice stability is affected by the alloy elements. It has been shown that the presence of tungsten and molybdenum stabilizes the superlattice while the presence of cobalt has a negative effect on the stability of the structure.

The degree of long range ordering and the kinetics depend on the aging temperature and the composition. By increasing the aging temperature nucleation rate decreases while the grain growth rate will increase. The maximum kinetics is obtained for the composition Ni_2Cr. The larger deviation from the stoichiometry the slower kinetics of LRO is obtained. The presence of tungsten and molybdenum will have an accelerating effect on the order kinetics. On the other hand, the kinetics is strongly subdued by the presence of cobalt and iron.

Nath et al. [27] showed that the kinetics of lattice contraction affected by the aging time and applied strain. They concluded the results from their lattice contraction measurements for Nimonic 80A shows that, the contraction is divided in three stages. During the first 500 h the contraction rate was high. During the next 15 000 h it became very slow and then it accelerated again at longer aging time.

2.7.3 Negative creep

The term negative creep is generally used for the superposition of two opposite processes. Common plastic creep process represents the positive component and lattice contraction process due to ordering represents the negative component. Superalloys show the negative creep as a contraction during creep test or as an increase in stress during relaxation test [26].

It has been also shown [26] that the ordering of Ni_2Cr in the form SRO and LRO arisen during aging at 550°C and below is responsible of lattice contraction. This phenomenon leads to dimensional instability and negative creep in Nimonic 80A and the binary alloy Ni-20wt%Cr. This was also confirmed that the presence of the precipitation of γ' had no effect on the process.

CHAPTER 3 EXPERIMENTAL PROCEDURE

3.1 DIMENSION OF INCONEL TENSILE SPECIMEN

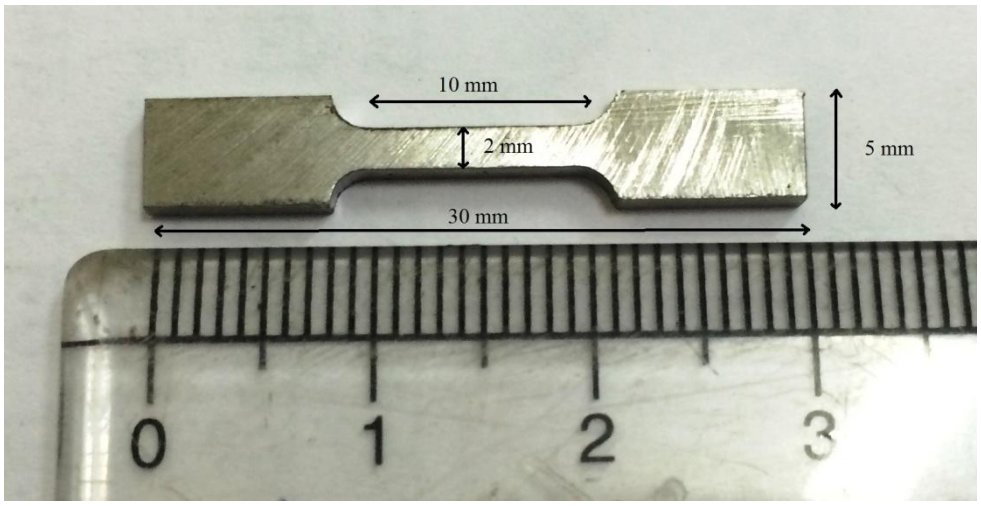

3.2 CHEMICAL COMPOSITION OF INCONEL 718

Table 1: chemical composition in weight percent

Ni	Cr	Fe	Nb	Mo	Ti	Al
53.5	19	18.5	4.5	3	1	0.5

3.3 AGING TREATMENT

To study the aging effect of Inconel 718 three specimens are analyzed at different conditions. First one is studied at no aging condition or as received sample and other two are as heat treatment specimen HT1 and HT2 aged at different conditions. HT1 and HT2 first both solid solutionized at 955ºC for 1hr/AC and the aging conditions are given below in table 2:

Table 2: Heat treatment process of HT1 and HT2 specimens

HT1	• 955ºC for 1hr; air cool to RT • 718ºC for 8hr; furnace cool to 621ºC • 621ºC for 18hr; air cool to RT
HT2	• 955ºC for 1hr; air cool to RT • 718ºC for 8hr; air cool to RT

3.4 LIGHT OPTICAL MICROSCOPE

Figure 11: Lieca optical microscope

The metallographic analyses were carried out before and after the aging heat treatment. The samples were carefully polished on emery paper in decreasing order of coarseness successively using 100, 320, 900, 1200 and 1500 grit Sic paper. The grinded surface of the specimens was polished on colloidal silica contained velvet polishing cloth. To making visible the microstructure etching were done by using waterless kalling solution containing 5 g $CuCl_2$, 100 ml HCl and 100 ml ethanol on the polished surfaces for 30 to 40 seconds. Microscopic examination of the etched surface of specimens was successfully completed using a metallurgical digital microscope (Lieca) through which the resulting microstructure of the samples was all photographically recorded. For high resolution microstructures SEM and FESEM has also been used.

3.5 XRD

Figure 12: X-ray diffraction machine

In this technique we evaluate the precipitate phase present in the Inconel 718 such as γ, γ′, γ′′ and δ. The XRD scanning was done in the range of 30° to 110° and the scanning rate was 1° per minute. After that the graph was analyzed in X-pert high score software.

3.6 HARDNESS TEST EQUIPMENT

For hardness testing, the sample was grinded and polished and for heat treated sample oxide layer was removed. During this experiment 10 readings were taken at different positions from the sample. The parameters for the hardness test at which performed: load=10 kg and dwell time=10 sec.

Figure 13: Vickers hardness testing machine.

4.1 OPTICAL MICROSTRUCTURE OF AS RECEIVED

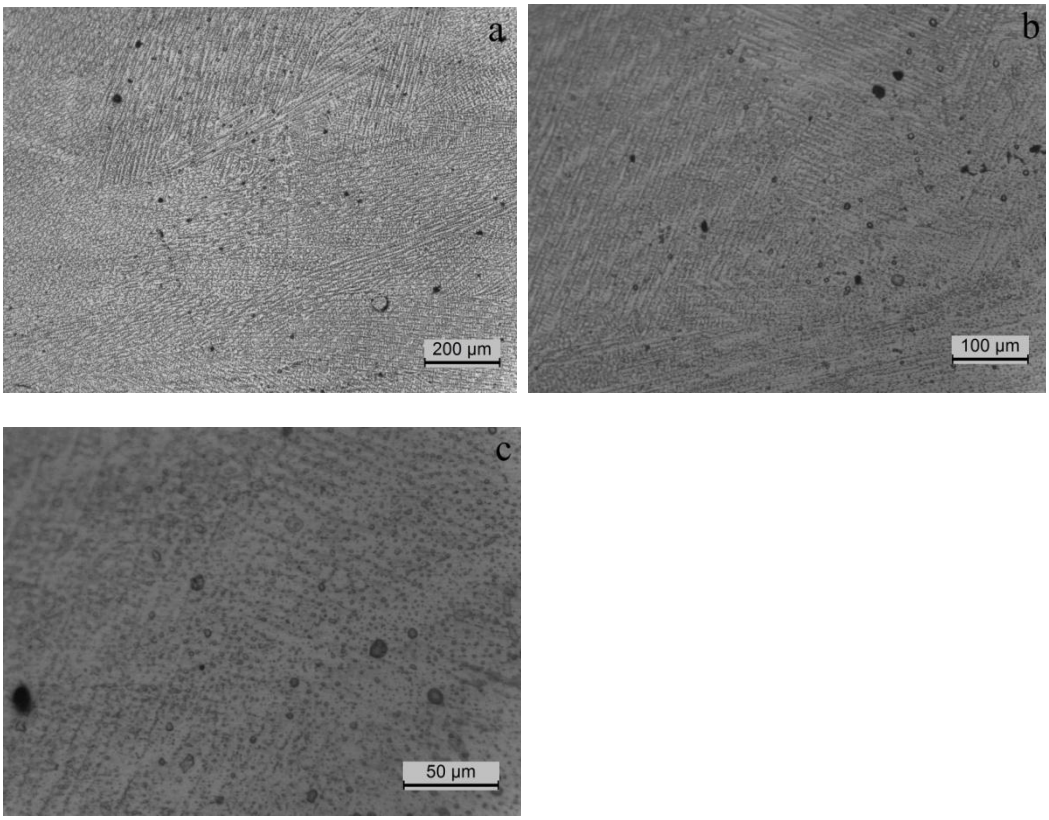

Figure 14: Optical microstructure of as received at 10x, 20x and 50x (fig.a,b,c)

The microstructure is showing that the laser scan pattern is bidirectional as we discussed above. The fig.14c, shows the zig-zag pattern during the deposition primary dendrites grow at the angle of +45° and -45°. There is no precipitate phase present in the microstructure clearly shown.

4.2 OPTICAL MICROSTRUCTURE OF SINGLE STAGE AGING(HT2)

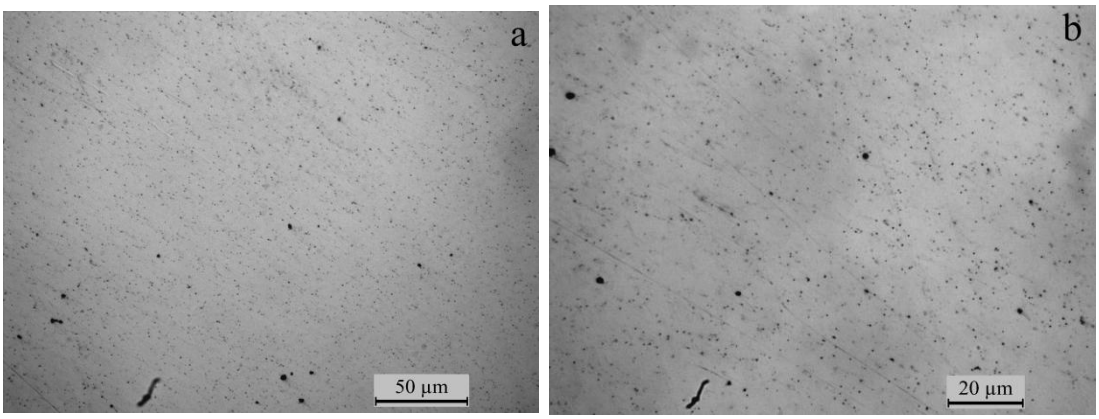

Figure 15: Optical microstructure of single stage aging at 50x, 100x(a,b)

Above fig.16 (a,b) showing there is no grain boundaries present in the microstructure. XRD shows some precipitate $Fe_{0.64}Ni_{0.36}$ and $Cr_{.19}Fe_{.70}Ni_{.11}$ present in the matrix.

4.3 OPTICAL MICROSTRUCTURE OF TWO STAGE AGING(HT1)

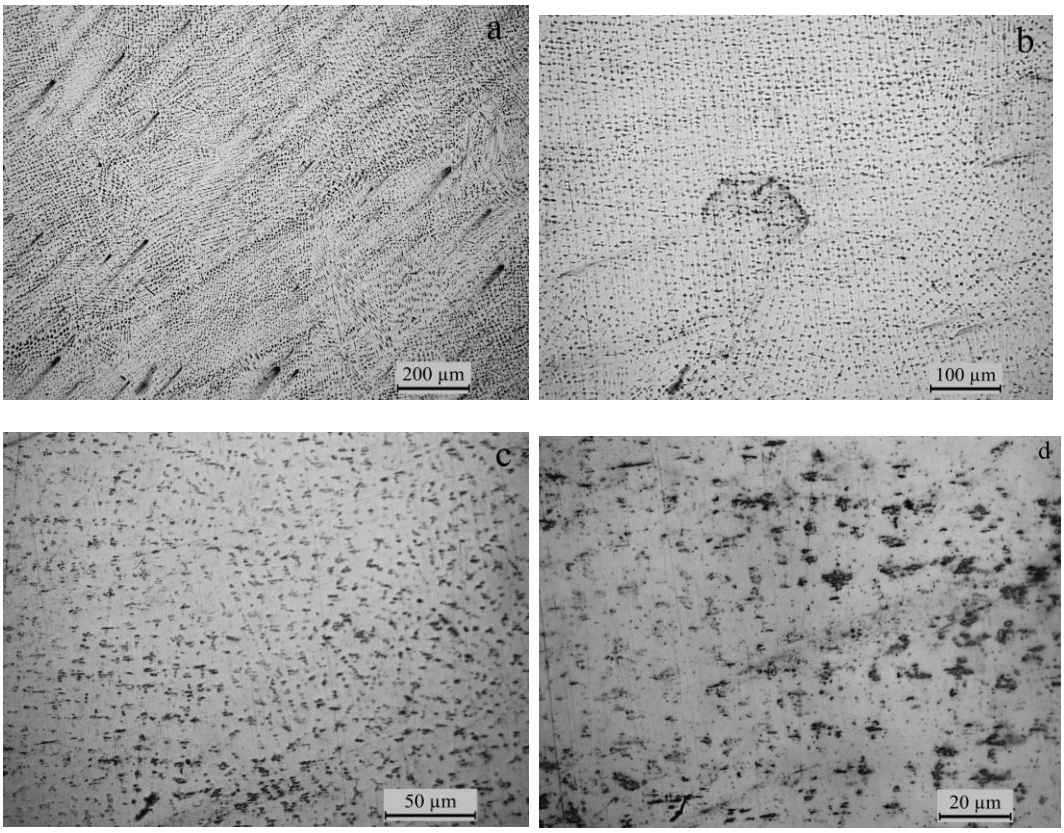

Figure 16: Optical microstructure of two stage at 10x, 20x, 50x and 100x(fig.a,b,c,d)

Two stage aging images shown in fig.17 at different and lower magnification, they are showing dendritic growth. During aging for longer time the grain growth is possible because in hardness test showing less hardness then the single stage.

4.4 SEM MICROSTRUCTURE OF AS RECEIVED

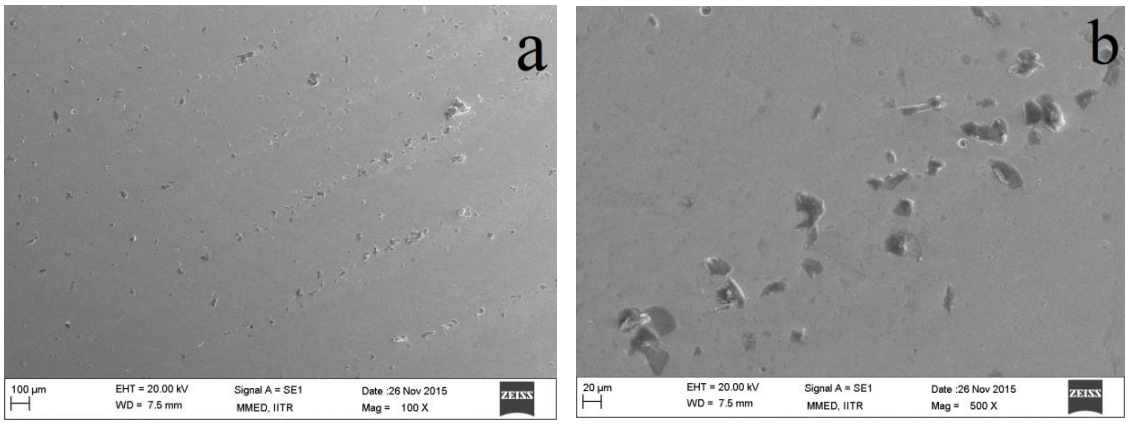

Figure 17: SEM images of as received at 100x and 500x(a,b)

The fig.18 shows the SEM images of as received inconel 718 at lower magnification, because at higher magnification there was no phase or precipitate particles to shown. At lower magnification some particles are visible but confirmed unless done XRD of as received sample.

4.5 SEM MICROSTRUCTURE OF HT2

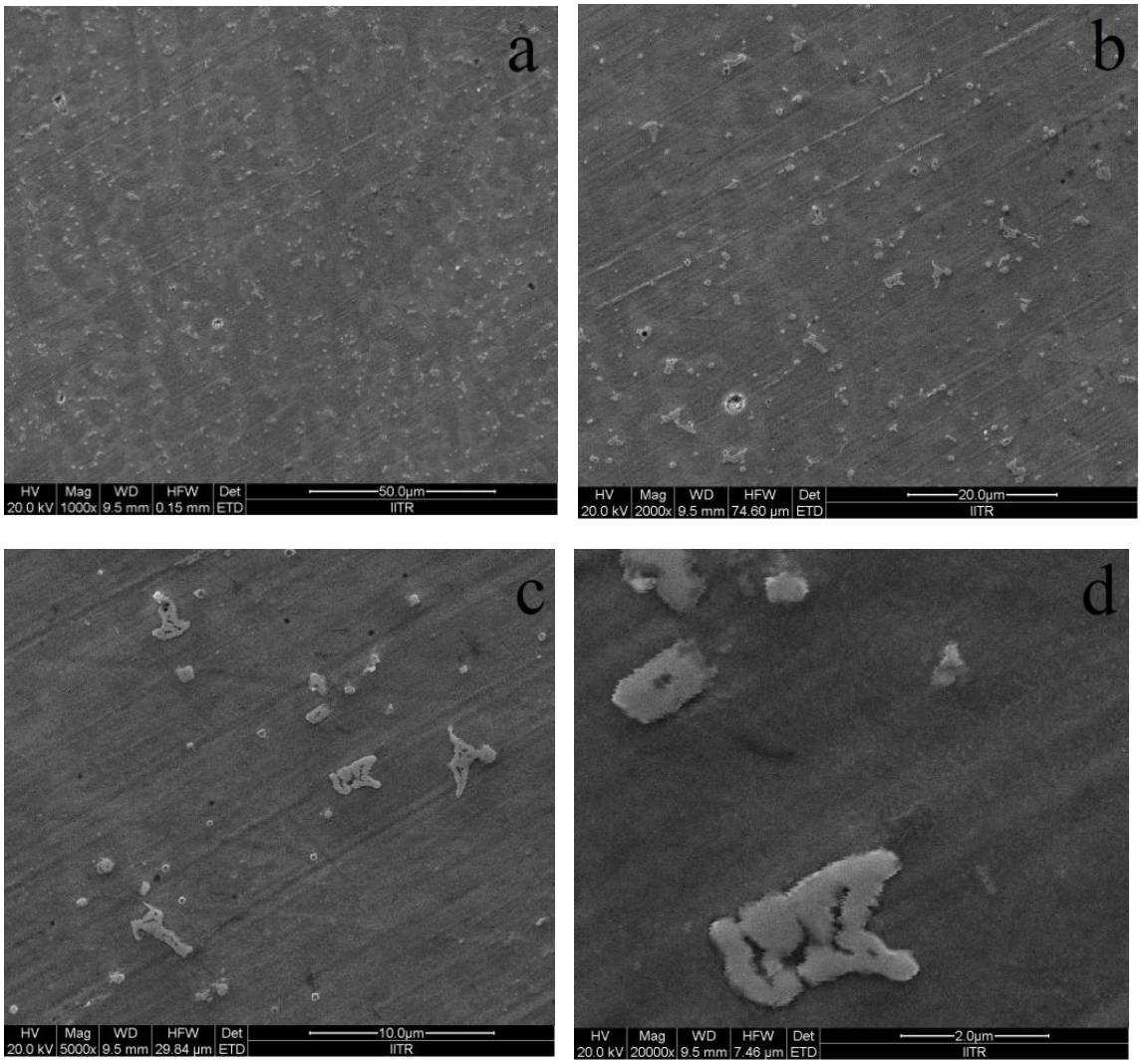

Figure 18: SEM images of single stage aging 1Kx, 2Kx, 5Kx, 20Kx(a,b,c,d)

According to above fig.19 shows the precipitate forms in single stage aging and distributed uniformly in the matrix. These precipitates are responsible for the increase in hardness.

4.6 SEM MICROSTRUCTURE OF HT1

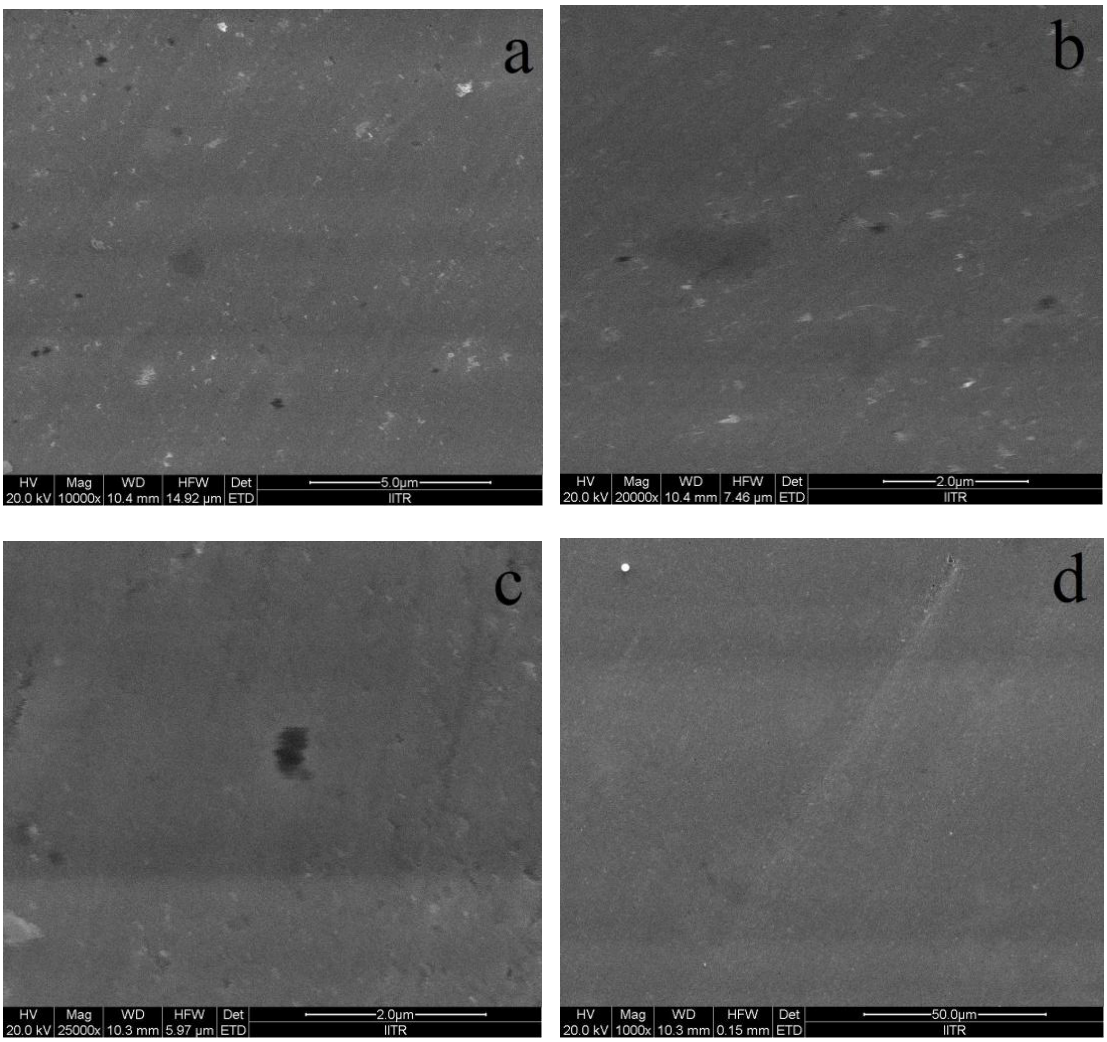

Figure 19: SEM images of two stage aging at 10Kx, 20Kx, 25Kx and 1Kx(a,b,c,d)

The microstructure of two stage aging shown in fig.20, due to aging 26 hr the precipitate forms but precipitates grow and dissolve again in matrix. So we can hardly see some precipitates in the microstructure but XRD clarify that presents of precipitate.

4.7 PHASE ANALYSES

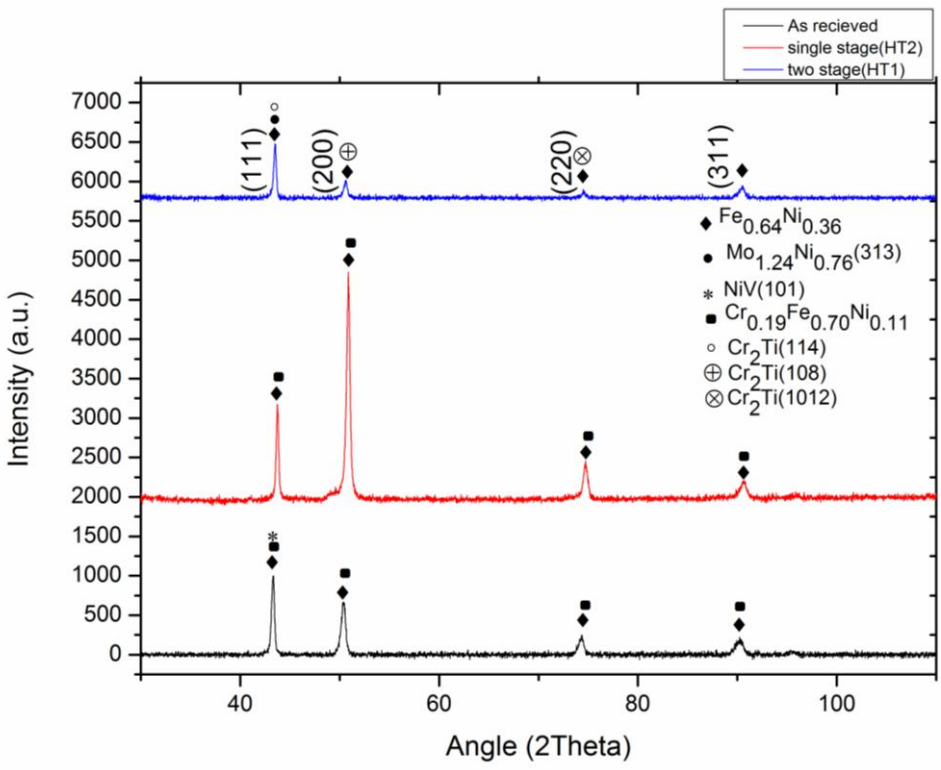

Figure 20: Phases present in all specimens showing with symbols

The XRD analyses showing the phases present in the as received, HT2 and HT1. The $Fe_{0.64}Ni_{0.36}$ is present in all the samples so we can consider it as matrix phase. At single stage aging $Cr_{.19}Fe_{.70}Ni_{.11}$ precipitate forms which increase the hardness and strength, while in single stage aging there is present $Mo_{1.24}Ni_{0.76}$ (δ) phase which is orthorhombic crystal structure. This phase is softer and reduces in hardness.

4.8 VICKERS HARDNESS TEST

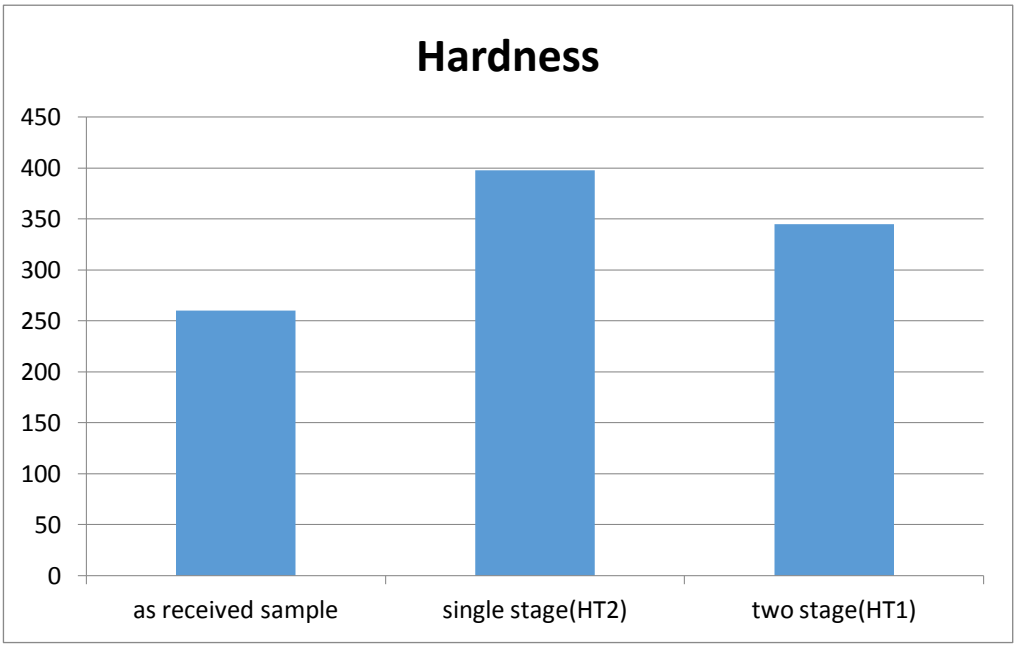

Figure 21: Hardness values of specimens in VHN

According to above fig. 17, showing the average hardness of as received specimen as 260.2 VHN. After heat treatment of HT2 and HT1 show the hardness increases 397.8 VHN and 345 VHN respectively. Single stage aging(HT2) shows the increase in hardness by 34%, due to precipitate forms, while two stage aging(HT1) shows the less increase in hardness because of the formation of acicular phases.

4.9 TENSILE TEST RESULT

Table 3: Results of tensile tests of age hardened samples compared with as-received sample of Inconel 718

specimens	0.2% Yield stress (proof stress) (MPa)	Ultimate tensile stress (MPa)	Fracture stress(MPa)
As received	521.79	810	801
Single stage(HT2)	904.04	1083.75	1077.5
Two stage(HT1)	976.46	1125	1111.25

The breaking point of the specimens is at the middle, so results of the tensile tests are valid. Differences in the tensile properties are influence by the crystallographic texture and the distribution of the precipitates. As shown in table 2, two stage aging specimen get higher stress values then single stage aging, but relatively low plastic elongation.

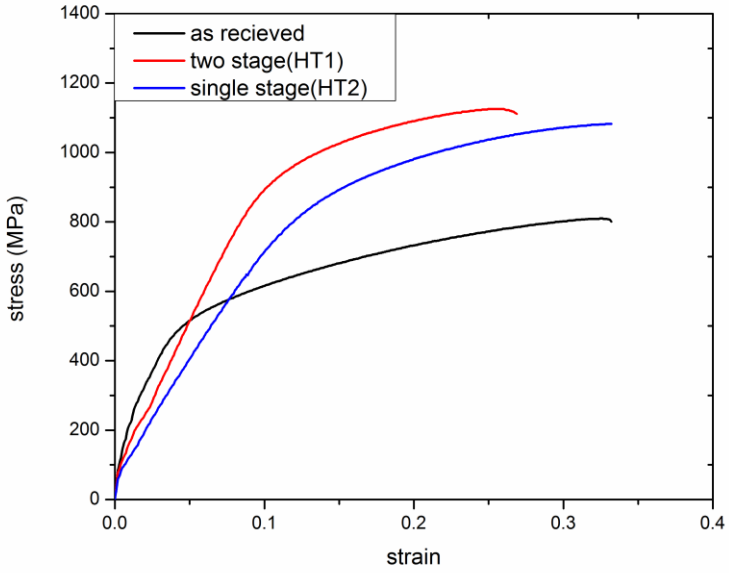

Figure 22: Stress-strain curves of as received, single stage and two stage aging specimens

4.10 CONCLUSIONS

The optical microstructure shows the pattern of the laser processing is bidirectional. This In718 single crystal or directionally solidified is deposited on the polycrystalline stainless steel substrate. Directionally solidified component is very hard to deposit on the polycrystalline substrate. The SEM microstructure shows the presence of more precipitate in single stage then two stage aging. It means for longer time of aging some phases dissolve or show growth.

XRD analyses confirm the presence of precipitates in the different aging conditions. Two stage aging shows the acicular phase, which arise after the long time aging and softer phase.

With the aging time hardness increases but after a certain time period the hardness starts decreases. HT2 showing higher hardness then the HT1 because of the absence of the (δ) delta phase.

Stress-strain curve in elastic region or modulus of elasticity changes after heat treatment. The strength of two stage aging sample is higher than the single stage but the reduction in ductility. This can be related by the phase formation after the heat treatment.

4.11 FUTURE SCOPE OF WORK

No signs of corrosion were seen in the samples even after prolonged exposure to atmospheric conditions. This might be an indication of enhanced corrosion resistance. Corrosion studies should be carried out in order to get a deep inside for this property.

High temperature tensile can be conducted after aging about 650° C to find out the changes in mechanical properties and microstructure.

Inconel 718 generally used for high temperature applications such as gas turbine blades. At such high temperature applications creep is the dominant mode of failure so study creep behaviour should be carried out.

REFERENCES

[1] C.Slama and M.Abdellaoui, Structural characterization of the aged Inconel 718, Journal of Alloys and Compounds 306, 277-284, 2002.

[2] W. Sims, C., Stoloff, N., Hagel, Superalloys II, October,19 ed. (Intersceince, Wiley, n.d.), pp. 615.

[3] J. Davis: Heat Resistant Materials, Wiley-interscience, pp.589-591,1997.

[4] J. Saarimäki: The Mechanical Properties of Lattice Truss Structures with Load-Bearing Shells Made of Selectively Laser Melted Hastelloy XTM, KTH, 2011.

[5] R.C.Reed: The Superalloys (Cambridge University Press, Cambridge, UK, 2006),pp. 370-372, 2012

[6] M.Dehmas, J.Lacaze, A.Niang, and B.Viguier, TEM Study of high temperature precipitation of Delta phase in Inconel 718 alloy, Advances in Material Science and Engineering, 2011.

[7] Davis, J.R.: Heat resistant Materials. Materials Park: ASM International,1997.

[8] Sims, C.T., Stoloff, N.S., Hagel, W.C: superalloys *II*. New York: Wiley-interscience,1987.

[9]. Donachie, M.J., Donachie, S.J.: Superalloys. A Technical Guide. 2nd edition. Materials Park: ASM International.2002.

[10]. Orakzai, K.: Effect of Carbon Content on the Properties of CMSX-4. Finspång: Siemens Industrial Turbomachinery AB, 2004.

[11] G.P. Dinda, A.K. Dasgupta and J. Mazumder: Texture control during laser deposition of nickel-based superalloy, Scripta Materialia,vol.67,pp.503–506, 2012.

[12] C.-M. Kuo, Y.T. Yang, H.Y. Bor, C.-N.Wei, C.-C. Tai:Aging effects on the microstructure and creep behavior of Inconel 718 superalloy, Materials Science and Engineering,pp.289–294,2009.

[13] I.Tabernero, A.Lamikiz, S.Martı´nez: Evaluation of the mechanical properties of Inconel 718 components built by laser cladding, International Journal of Machine Tools & Manufacture,pp. 465–470,2011.

[14] Xiaoming Zhao, Jing Chen, Xin Lin: Study on microstructure and mechanical properties of laser rapid forming Inconel 718, Material science and engineering,vol.478,pp.119-124,2008.

[15] J. J. Valencia, T. McCabe, K. Hensl, J. 0. Hansenz, and A. Bose: Microstructure and mechanical properties of inconel 625 and 718 alloys processed by powder injection molding, The Minerals, Metals &Materials Society,PP.936-944,1994.

[16] W. D. Cao: Superalloys 7 18. 625 and Various Derivatives, edited by E. Loria,pp 147-160,1991

[17] Bi GJ, Gasser A, Wissenbach K, Drenker A, Poprawe R: Investigation on the direct laser metallic powder deposition process via temperature measurement,Appl. Surf. Sci,pp.253-261,2006.

[18] Liu JC, Li LJ: In-time motion adjustment in laser cladding manufacturing process for improving dimensional accuracy and surface finish of the formed part, Opt. Laser Technol,vol.36(6),pp.477–83,2004.

[19] Lewis GK, Schlienger E.: Practical considerations and capabilities for laser assisted direct metal deposition, Mater. Des. ,vol.21(4),pp.417–23,2000.

[20] Wu X, Mei J.: Near net shape manufacturing of components using direct laser fabrication technology, J. Mater. Process Technol,vol.13(2-3),pp.266–70,2003.

[21] C.P. Paul, P. Ganesh, S.K. Mishra, P. Bhargava, J. Negi, A.K. Nath: Investigating laser rapid manufacturing for Inconel-718 components, Optics and Laser Technology,pp. 800–805,2007.

[22] X. Zhao, J. Chen, X. Lin, W. Huang: Study on microstructure and mechanical properties of laser rapid forming Inconel 718, Materials Science and Engineering,pp.119–124,2008.

[23] D. Clarka, M.R. Bacheb, M.T. Whittakerb: Shaped metal deposition of a nickel alloy for aero engine applications, Journal of Materials Processing Technology,pp.439–448,2008.

[24] D. Dudzinski, A. Devillez, A. Moufki, D. Larrouquere, V. Zerrouki, J. Vigneau: A review of developments towards dry and high speed machining of Inconel 718 alloy, International Journal of Machine Tools and Manufacture ,vol.44,pp. 439–456,2004.

[25] F. Liu, X. Lin, G. Yang, M. Song, J. Chen, W. Huang: Microstructure and residual stress of laser rapid formed Inconel 718 nickel-base superalloy, Optics and Laser Technology,vol.43,pp. 208–213,2011.

[26] Moverare, J.: Shrinkage and ageing of Ni-base alloys at intermediate temperatures (400-600C),pp.358-367,2005.

[27] Marucco, A., Nath, B.: Effects of ordering on the properties of Ni-Cr alloys. J.Mat. Sci., 23, pp.2107-2114,1988.

[28] Rtishchev, V.V.: Structure transformations and property changes of Ni- base superalloys on ageing. Mat. Adv. Power Enf.,(1), pp.889-898,1994

Turnitin Originality Report

Aging behavior of Inconal 718 prepared by laser processing by Ajay Singh Tomar

From saurabh (dash)

Processed on 26-May-2016 17:19 IST
ID: 678565524
Word Count: 7402

Similarity Index	Similarity by Source	
14%	Internet Sources:	7%
	Publications:	6%
	Student Papers:	1%

sources:

1 6% match (Internet from 18-Sep-2015)

http://www.ewp.rpi.edu/hartford/users/papers/engr/ernesto/morens/EP/References/Ageing%20Infl%20uence%20on%20based.pdf

2 4% match (publications)

Dinda, G.P., A.K. Dasgupta, and J. Mazumder. "Texture control during laser deposition of nickel-based superalloy", Scripta Materialia, 2012.

3 1% match (Internet from 20-Apr-2014)

http://www.coursehero.com/file/8520643/SokalRohlfIntroductionBiostatistics2ed1987/

4 < 1% match (publications)

Wang, Xiaoqing, Xibing Gong, and Kevin Chou. "Review on Powder-Bed Laser Additive Manufacturing of Inconel 718 Parts", Volume 1 Processing, 2015.

5 < 1% match (publications)

Kuo, C.M.. "Aging effects on the microstructure and creep behavior of Inconel 718 superalloy", Materials Science & Engineering A, 20090615

6 < 1% match (student papers from 13-Dec-2012)

Submitted to Cranfield University on 2012-12-13

7 < 1% match (Internet from 07-Jan-2016)

http://eis.ktu.lt/index.php/Mech/article/download/4149/2475

8 < 1% match (publications)

Valle, L. C. M., L. S. Araújo, S. B. Gabriel, J. Dille, and L. H. de Almeida. "The Effect of δ Phase on the Mechanical Properties of an Inconel 718 Superalloy", Journal of Materials Engineering and Performance, 2013.

9 < 1% match (publications)

Carton, Marc, Ennis, Philip James, Lecomte-Beckers, Jacqueline and Schubert, Florian. "Materials for Advanced Power Engineering 2006", Forschungszentrum Jülich, Zentralbibliothek, Verlag, 2007.

10 < 1% match (publications)

Gong, Xibing, Xiaoqing Wang, Vernon Cole, Zachary Jones, Kenneth Cooper, and Kevin Chou. "Characterization of Microstructure and Mechanical Property of Inconel 718 From

Selective Laser Melting", Volume 1 Processing, 2015.

11 < 1% match (publications)
A. Rokanopoulou. "Titanium carbide/duplex stainless steel (DSS) metal matrix composite coatings prepared by the plasma transferred arc (PTA) technique: microstructure and wear properties", Journal of Coatings Technology and Research, 07/13/2010

12 < 1% match (Internet from 24-May-2016)
https://ecommons.usask.ca/bitstream/handle/10388/etd-11172006-133611/Dubiel.pdf?isAllowed=y&sequence=1

13 < 1% match (publications)
Fencheng Liu. "Effect of intermediate heat treatment temperature on microstructure and notch sensitivity of laser solid formed Inconel 718 superalloy", Journal of Wuhan University of Technology-Mater Sci Ed, 10/2011

14 < 1% match (publications)
Brian Gleeson. "High-Temperature Corrosion of Metallic Alloys and Coatings", Materials Science and Technology A Comprehensive Treatment, 03/03/2000

paper text:

ABSTRACT The

13**inconel 718 is a** commercially successful **nickel-base superalloy widely used in**

nuclear reactors, heavy machinery

2**and other high-temperature applications because of its good corrosion resistance, mechanical properties and structural stability up to 650º**

C. for high temperature application directionally solidified or single crystal is used because of

2**its better creep resistance and** thermo-mechanical **fatigue behavior in the absence of grain boundaries.** But **the** manufacturing cost **of single crystal is**

more this is one of the major problems. Hence, there developed interest in finding an alternative route synthesizing inconel 718 by laser deposition on mild steel substrate. An intense laser heating of the powder feed followed by cooling of the metal powders (via substrate) leads to a dendritic microstructure in layer wise growth of the material: this subsequently gets exposed to further heating during multilayer growth of the material up to 28 mm in length and 15 mm in thickness. As it is known, precipitation of inter-metallic phases during heat treatment improves creep resistance in inconel 718. Prior to this, a solutionizing treatment is also necessary at 955ºC for 1 hr. Thus, a microstructure comparison of the as-prepared sample was done with respect to the samples heat treated at 718ºC for 8h (HT2) and another at 718ºC for 8h+ 621ºC for 18 h (HT1), as commercial practice. CHAPTER 1 INTRODUCTION 1.1 Introduction Superalloys, as the name implies have characteristics that make them different from other materials. Modern superalloys consist multiple elements, may be more than 14 elements. This makes them different entity from the past alloys which can be dominated by one element. If we look our past we

can realize that materials have a dominant impression on our civilizations. These materials have a direct or indirect effect on the culture, tradition, and daily life.

> 5**Inconel 718, nickel-base .superalloy, was developed** b.y **International Nickel Corporation**

i.n t.he

> 5**1950s and found many applications in turbine** and aero engine **components.**

Nickel-based superalloys have lot of development during

> 10**over the** last **four decades. Inconel** 7.18, **a Ni-Cr-Fe superalloy,** h.as **been** used **in**

m.any a.pplications s.uch as gas turbine .blades, aero engine, nuclear r.eactors due to its excellent properties as corrosion resistance, creep resistance and oxidation .resistance, thermal fatigue, also easiness of

> 5**forging, welding and brazing,** are **the advantages of Inconel 718.**

Inconel 718 c.an retain its

> 4**mechanical properties in a range of**

temperature due to s.olid-solution strengthening and p.recipitation s.trengthening.

> 4**Nevertheless, its .high .hardness and low .thermal conductivity** c.haracteristics **.make it difficult .to apply .conventional** m.achining **.methods**

> 4**.because of tool** o.ver **-wear .and poor .work-piece surface**

i.ntegrity [1] [3]. According to, high temperature materials should possess the following characteristics:- I.

> 6**Ability to withstand loading at an operating temperature close to its melting point.** II. **A substantial resistance to mechanical degradation over extended** period **of time.** III. **Tolerance of** sever **operating environments.**

These high temperature materials commonly called superalloys are developed to face the challenges of efficient energy demands but at the same time minimizing greenhouse gas emissions. 1.2 Types of superalloys There are various superalloys developed by several industries, which have different

application in aero industry, power generation and nuclear power plants etc. They are available in cast (usually heat treated or otherwise processed) or wrought (often heat treated or otherwise processed) forms. The chemical composition of each of them varies, based on the desired characteristics. The current superalloys are usually consists of 10 to 15 elements. But there are three main categories that are jointly called superalloys as mentioned below. They possess high level of temperature insensitivity or stability and are widely used as base materials for high temperature applications. 1. Nickel base superalloy 2. Iron-nickel superalloy 3. Cobalt base superalloys Inconel 718 superalloy is a family of austenitic nickel-chromium base superalloy. These alloys are generally used at temperature above 450 °C, as at these temperatures ordinary steel and titanium alloys are losing their strengths; also corrosion is common in steels at this temperature. 1. Nickel based superalloys: The solid solution γ phase constitutes the Ni phase, which has a Face Centered Cubic (FCC) crystal structure [1]. Usually used when high strength is the required, for the temperature range of 1024º to 1371 °C. They are a widely used and renowned group of austenitic alloys. The unique characteristic of this group of superalloys are their application without compromising their integrity close to their melting temperatures. Ni-base superalloys can be divided into three types: a. Solid solution strengthened alloys: which usually contains the following alloying elements; Fe, Co, Cr, Mo, W, Ti, Nb and Al. Such as Haynes230 and HasteloyX. Among these Al, Cr, W and Mo are potential solid–solution strengtheners because of different atomic radius as compared to Ni [2]. They are more suitable for processing, for example weldability [3] and can also be manufactured into complex geometries from powders using laser melting techniques as described in [4]. b. Precipitation (age) hardened alloys: usually contain Al, Ti, Ta and sometimes Nb that facilitate the formation of γ′ and γ″ precipitates in the γ matrix. Such as Inconel 718, 738, 939 and Wasp alloy. it is evident that precipitation hardened alloys possess higher strengths compared to solid solution strengthened alloys and are widely used in high temperature applications. c. Oxide dispersion strengthened (ODS) alloys: alloys contain fine oxide particles of Y2O3 about 0.5 to 1%. 2. Nickel-iron superalloys: The most important class of this group are t.hose alloys t.hat are s.trengthened by .an intermetallic .compound p.recipitation in an .FCC m.atrix. The common precipitate is γ′ [5]. Alloys such as Inconel 718, which has γ′ and γ″ precipitates are classed as iron-nickel base because of their higher percentage of Fe, but are considered to be nickel based. Others superalloys in this group consist of stainless steel strengthened by solid-solution hardening. They are primarily used as a wrought material and are comparatively cheaper than Ni base alloys. 3. Cobalt based superalloy: are strengthened by the c.ombination of .carbides and s.olid s.olution hardeners. Cobalt crystallizes in the Hexagonal closed packed (HCP) crystal structure below 417°C, as shown in the figure 1. They p.ossess e.xcellent c.orrosion resistance at high temperatures (980-1100 °C) b.ecause of t.heir h.igher c.hromium .contents. They p.ossess .better weldability and t.hermal f.atigue .resistance as .compared to n.ickel .based alloy. But cobalt-base alloys are more likely to precipitate undesirable sigma (σ) and Topological Closed Packed (TCP) phases. Depending on the application / composition involved it may be wrought or cast. Figure 1: HCP structure of cobalt 1.3 Physical metallurgy of nickel and its alloys Nickel is the fifth rarest element on earth and has a

12**Face Centered Cubic (FCC) crystal structure** as **shown in figure 2.**

It belongs to the family of transition metals and exists in the form of five stable isotopes. Transition elements are often called transition metals (possess the properties of metals) or d-block elements, includes group 3-12 in the periodic table. The elements that are alloyed with Ni to form superalloys and the phases they contribute to also is mentioned in the figure 2. Figure 2: Elements added in Ni to form superalloys The melting temperature is ~ 1455 °C and has a density of 8907 kg/m3 at room temperature. The characteristic that give nickel excellent mechanical properties even at high temperature is its negligible yield strength / temperature sensitivity. Another reason is that the FCC crystal structure that is both tough (toughness is the measure of resistance to fracture which is measured in units of energy) and ductile because of the c.ohesive .energy a.rising from t.he b.onding .provided by the .outer electrons. Secondly, Ni is s.table in its austenitic f.orm temperature to its .melting p.oint (i-e no p.hase t.ransformation). Also low diffusion rate in FCC metals give good micro-structural stability even at very

high temperatures [5]. Figure 3: FCC structure of Ni Ni based superalloys belongs to the family of austenitic nickel- chromium based superalloys that typically contains 80% Ni and 20% Cr. Several alloying elements are included in different percentages depending on the need to achieve better mechanical properties. Ni- based alloys are usually strengthened by precipitation (age) hardeners, they may

14**be wrought or cast depending on the application / composition involved.**

The modern complex superalloy composition is due to unique phase chemistry and structure. The microstructure consists of different phases. The important ones such as gamma .phase (γ), g.amma .prime (γ′), g.amma .double .prime (γ″), delta .phase (δ) and various carbides and borides are explained below. ? The gamma phase (γ): The gamma phase is the matrix phase of nickel-based superalloys in which the other phases reside. It exhibits a FCC crystal structure and its composition mainly consist of Ni with other elements such as Co, Cr, Mo, Ru, Re, and Fe [5]. ? Gamma .prime (γ′): forms the p.recipitate p.hase, w.hich is .usually c.oherent w.ith the γ.-matrix and is t.he main strengthening precipitate in nickel based superalloys. Similar to the γ phase γ′ have an ordered FCC crystal structure. γ′ mainly consist of Ni, Al, Ti, and Ta i-e Ni3(Al,Ti) [5]. ? Gamma double prime (γ″): is a strong coherent metastable precipitate with a body center tetragonal (BCT) structure, it is the primary strengthening precipitate. The γ″ unit cell precipitate i.e. Ni3Nb consists of Ni and Nb is shown in figure 3 [1], is usually found in Ni-Fe superalloys. At higher temperature γ″ become unstable and can transform into δ phase [6]. Figure 4: BCT structure of gamma double prime (γ″) ? Delta phase (δ): is a non-hardening precipitate usually present at grain boundaries. The loss of hardening is due to depletion of γ″. The structure is orthorhombic and the δ phase improves the creep rupture and grain boundary sliding resistance. It is composed mainly of Ni, Nb and Ti. ? Carbides and borides: Carbide usually forms when carbon reacts with Ti, Ta and Hf and result in MC carbides. Where M represents elements such as Cr, Mo, Ti, Ta, or Hf. The MC carbides break-down during service to other species, such as M23C6, M6C, M7C3, and M3B2. These decomposed compounds usually reside in the γ grain boundaries [5]. Borides are found in superalloy in the form of M3B2, having a tetragonal unit cell, Which is also present in grain boundaries and improve the creep rupture resistance of superalloys [3]. Other phases: For example TCP, μ, σ, and laves etc. are present in the form of plates and needles. Under some conditions these can result in lower rupture strength and increase the creep rupture strength [35]. Although it is not desirable to have these compounds. CHAPTER 2 LITERATURE REVIEW 2.1 LASER PROCESSING Laser processing is also termed as l.aser .metal d.eposition, selective l.aser .melting or direct .metal .deposition, which can produce three-dimensional parts by using CAD/CAM software. These techniques are being used in various industries for manufacturing, repair, layer by layer net like structures. The main advantages of laser metal deposition are lead time and minimization of waste material. Plasma welding is having high deposition rate than laser metal deposition, but it can produce better coating, with less distortion with sound surface finish. So laser technique is used for costly material parts. [11] [13]. Laser metal deposition is a new arising laser manufacturing technology that added laser manufacturing with quick models making and form

2**a solid freeform fabrication process.** Laser metal deposition **has the** ability **to control the temperature of the**

melted pool, dimensional accuracy and composition of the deposit metal. This process has been developed in many industries and laboratories by the different names such as laser powder melting technique or laser net shaping technique, but the basic principles is same in all the technologies.

2**A high-power laser beam** is used **to create a melt pool** of **the** powder **which is delivered**

by the tiny holes to create metal pool on the substrate metal. A computer numerical control system or computer-aided design

2**system is used to control the** laser beam **motion** and **the**

path of the tool according to the three-dimensional object we want to create, laser beam create the component layer by layer[16] [18]. Figure 5: Schematic diagram of laser processing Direct metal deposition (DMD), due to its importance to create a dense part, flexibility in feed rate and shape precision, has been accepted as a promising manufacturing technique. By laser metal deposition, the geometrically complex shape and high dimensional accuracy can be achieved without doing any subsequent process which is not possible in conventional methods. The required microstructures of direct metal deposition (DMD) processed parts are definitely affected by the physical and chemical reaction occurs in melt pool and these reactions lead to non- equilibrium process of laser technique. So there is lot of research efforts are required to optimize the laser parameters to get desired microstructure and mechanical properties of fabricated components [11] [12]. 2.2 DEVELOPMENT OF INCONEL 718 BY LASER PROCESSING A laser metal deposition system w.hich was developed in

2**.University of Michigan** u.sed **to** create **two types of** sample **A and B, with different laser scanning patterns**

uni-axial and bi-axial which s.chematically shown in fig.6 [11]. A 6 kW CO2 laser w.ith a s.pot s.ize of 0.5 mm u.sed in t.his .experiment INCONEL 718 powder w.as used in t.his experiment and the mesh sizes of the powder particles was -100 to +325. The

2**powder had a composition of 53.5 Ni, 19 Cr, 18 Fe, 5 Nb, 3 Mo, 1 Ti and 0.5 Al in** weight%. **Laser deposition parameters (laser power:** 750 watts, **scanning speed: 6.**

25 mm/s; powder feed rate: 0.2 g/s) was

2**kept constant for both deposits. To prevent the melt pool from oxidation, helium was used as a shielding, as well as a powder carrier gas. Two** 50 mm **long and 3.** 2 mm **high deposits were made by successive deposition of 16 layers on a polycrystalline** Inconel 718 **rolled plate of dimensions**

100 mm ×30 mm ×15 mm. The laser deposition d.irection of all l.ayers was same

2**(left to right) in deposit A.** While, **a** forward **and** backward **deposition pattern was used** to create **deposit B.**

In this d.eposition .pattern l.aser s.can is .altered by 180º from the p.revious layer [11] [16]. Figure 6:

2**Optical micrographs of the as-deposited IN718 samples produced with two**

different laser beam scanning patterns

The primary dendrites growing direction are at an angle of 60º from the substrate. In deposit B, as we can see in Figure 6b ordered columnar dendrites are present in the longitudinal cross section. The

2**growth direction of primary dendrites** changing **in each layer by** 90º **with respect to the** primary dendrites **growth direction,** the growth direction **of primary dendrites**

is altered by +45º and -45º, corresponding to adjacent layers, respectively. Note that, even though for the

2**both deposits A and B the laser**

metal deposition parameters were constant, after that change in the

2**laser beam scanning pattern from unidirectional to bidirectional (backward and forward)** changes **the dendrite growth direction from** 60º **to** 45º. **In** direct metal deposition, **the** previously deposited layer **or**

substrate work

2**as a heat sink and heat flow**

in the one direction only. During solidification, primary dendrites always grow in the opposite direction

2**to the heat flow direction,** which is **perpendicular to the solid–liquid interface. Since the local heat flow is** always **unidirectional. and perpendicular to the solidification front.** So d.endrites **grow perpendicular to**

t.he solid-liquid front and form a c.olumnar dendritic s.tructure l.ocally. However, solidification of a m.aterial in the form o.f columnar dendrites d.oes not always make a single crystal structure. In columnar dendrites, the crystal growth is one axis orientation almost all dendrites, while other two axis remain free to grow. Hence, .columnar d.endrites can m.ake s.ingle grain .or poly grain .depending on the other .two axes o.f the d.endrites. Columnar d.endrite l.eads t.o a single c.rystal only w.hen all t.hree

2**.crystal axes of a dendrite are parallel to the corresponding. Crystal axes of all other dendrites in the sample.**

Figure 7: Metal deposition process in which metal is deposited over the substrate

2**To understand the** concept **of single crystallinity** and **polycrystallinity of**

a deposited metal by laser metal deposition, showing the

2**cross-sections** view **of deposits A and B, respectively** in figure 6. **The**

optical image of deposit A and B shows the dendrites orientation angle 60º

2**in deposit A and** 45º **in deposit B.**

it has been seen

2**that the morphology of the** grain growth **in deposit** A **is different from** deposit B. **In deposit A,** most of **the**

2**grains are aligned in** same **direction** and **the number of grains** in deposit A **is**

also higher than the deposit B. So we understand by this, bidirectional laser processing develops less grains compared to the unidirectional laser processing. So due to change in 90º growth direction the layers shows a zig-zag shaped pattern[14] [17] [23]. In FCC, [100] directions is having fastest rate of solidification. In g.eneral, s.olidification .occurs d.ue to the .nucleation a.nd .growth of .crystals. Solidification depends u.pon the c.onditions, .either n.ucleation or g.rain g.rowth .any .can be p.redominant. F.or e.xample, if .laser m.etal d.eposition i.s d.oing .on a .single c.rystalline s.ubstrate, which is .oriented in s.uch a .way t.hat a.ny o.ne of t.he [100] d.irections o.f t.hat s.ubstrate r.emain .parallel to .the l.ocal h.eat f.low d.irection, and t.hen s.olidification w.ill o.ccur o.nly in .the f.orm of .epitaxial g.rowth f.rom t.he .substrate. .Consequently, a. .single- crystalline .structure is m.aintained f.rom .the s.ubstrate t.o t.he c.lad. However, .when l.aser .cladding is c.onducted .on a p.olycrystalline s.ubstrate, o.nly .those g.rains o.f t.he s.ubstrate g.row .that h.ave a [100] .crystallographic .direction .that is p.arallel to t.he .local h.eat f.low .direction [11] [21]. In t.he case of b.idirectional l.aser m.etal d.eposition, t.he n.ucleation .and .growth m.echanism .is s.ame as i.n .the f.irst .layer of deposit A, .as mentioned .above. F.rom t.he s.econd l.ayer, due to the change in the laser scan pattern, t.here i.s a d.ifferent .process of n.ucleation and g.rain g.rowth. In this e.xperiment, p.rimary .dendrites .grew a..t a.n .angle of .about 60º t.o t.he .substrate .in .the f.irst l.ayer. .Due t.o t.he b.ackward .and f.orward l.aser b.eam .scan p.attern i.n d.eposit B., .the g.rowth .direction .of t.he p.rimary d.endrites i.s e.xpected .to c.hange b.y +60º .and -60º i.n t.he a.djacent .layers, respectively. .However, o.ptical m.icrograph (Fig. 6b) s.hows .that t.he d.endrite .growth .angle .was +45º .and -45º

3**i.n t.he s.** econd .layers .onwards. **T.his** 15º **c.**

hange i.n .dendrite .growth d.irection is t.he c.onsequence .of .the .preferred g.rowth

2**.direction .of FCC .crystal in .the [100] .directions.**

D.uring s.olidification .of F.CC .metals .and a.lloys, s.econdary .dendrites g.row p.erpendicular .to .the p.rimary d.endrites a.s t.he [100] d.irections are .perpendicular t.o e.ach o.ther. T.o .change t.he .dendrite g.rowth .direction b.y 60º .in s.ubsequent l.ayers, t.he n.ucleation o.f n.ew g.rains is r.equired a.t .the .layer

b.oundaries. H.owever, t.o .change t.he p.rimary d.endrite .growth .direction b.y 90º, n.o .nucleation i.s .required b.ecause t.he s.econdary d.endrites o.f .the .previous .layer c.an s.erve a.s a. g.rowth .front f.or t.he p.rimary d.endrites o.f .new l.ayer. I.n s.olidification, .the d.riving f.orce (free energy) r.equired f.or n.ucleation .is m.uch m.ore .than t.hat r.equired f.or .grain .growth. H.ence, i.n d.eposit B., t.he p.rimary .dendrite g.rowth d.irection .is a.ltered b.y 15º f.rom t.he h.eat f.low .direction t.o m.aintain t.he r.ight-angle r.elationship b.etween t.he p.rimary d.endrite .growth d.irection o.f .subsequent .layers .necessary t.o a.void a n.ucleation b.arrier. .Hence, .solidification o.ccurs mostly .by t.he e.pitaxial g.rowth .of .primary .dendrites .from

3**t.he s.** econdary **d.** endrites **.of p.** revious l.ayers **i.n**

d.eposit B. This .epitaxial g.rowth o.ccurs. f.rom t.hose g.rains w.hich h.ave a [100] d.irection o.riented.a.t a.n a.ngle of a.bout 45º. to t.he .layer i.nterface,

3**a.nd t.he** .growth **.of t.he** .other g.rains **c.**

eases.. As a r.esult, t.he .n.umber o.f .grains is d.ecreased .and t.he g.rains b.ecome l.arger at t.he u.pper p.art .of t.he c.lad. 2.3

1**DIRECTIONAL SOLIDIFICATION (DS) The directional solidification of superalloys was introduced** after **the sixties. In the directional solidification, the**

solidification direction and the grain boundaries are aligned parallel to each other. This alignment corresponds with the axis of the principal stress of that component. After the directional solidification the

1**final structure consist of** dendrite **grains** in **[001]** direction or **the direction of the load**

[21]. Stresses at higher temperature

1**have a** dominant **effect on the grain** boundaries which is **perpendicular to the stress direction.**

So, by aligning these grain boundaries can minimize the site of failures and the stresses on the superalloys can be reduced. Figure 8: Directionally solidified turbine blade Directionally solidified components have the creep resistance between the single crystal and the equiaxed grains. Directionally solidified turbine blades increase the thermal fatigue five times than the conventionally prepared turbine blades due to the orientation of grain boundaries at [001] direction of the applied stress [26]. 2.4 ADVANTAGE OF LASER PROCESSING Laser metal deposition is used in various applications, preparation of three dimensional components and repair applications. ? ? ? LMD reduces the waste material during manufacturing LMD reduces the cost of tooling which is higher in conventional methods LMD is used for parts repair which are costly to repair or very difficult to repair precisely ? It reduces the l.ead time of c.omponent ? Customization of parts on the fly ? LMD is used for deposition of novel metals ? Repair of mould tool surfaces ? LMD is used for making original part, hybrid manufacturing ? LMD provide easiness to the deposition of the reactive metals, without the use of protective atmosphere ? Used

for depositions of various materials such as Nickel base superalloy, titanium superalloy(Ti-6Al-V4) and also high strength steels ? Powder recycling methods for better process efficiency ? Deposition of metallic glasses and amorphous materials. ? LMD provides small voids or porosity, highly dense component can be produce ? Small heat affected zone ? LMD also provide high solidification rate The one of the best advantage of laser metal deposition is the ability to metal deposition for existing component for repair. Laser metal deposition also gives the facility for near net shape manufacturing which reduces waste material and tooling costs. 2.5 STRENGTHENING MECHANISMS Strengthening of s.uperalloys is essential f.or t.he .purpose o.f .obtaining t.he d.esirable h.igh- .temperature p.roperties. It can be o.btained t.hrough e.ither .solid-s.olution s.trengthening or .precipitation .hardening. Creep r.esistance i.s a.n e.xample o.f i.nteraction b.etween d.ifferent h.ardening m.echanisms. In e.arly s.tages o.f the .creep solid-solution strengthening is largest contributor effect on the creep resistance. The solid-solution effect decreases

1**with time .whereas the .contribution** of **the** p.recipitation **hardening increases.** 2.5 **.1 Solid solution strengthening** It **is**

h.eating o.f .an .alloy t.o an appropriate .temperature, h.olding i.t a.t t.hat t.emperature l.ong .enough t.o .cause .one o.r m.ore c.onstituents t.o .enter .into a s.olid s.olution .and .then .cooling .it r.apidly .enough t.o h.old t.hese c.onstituents i.n s.olution. .Subsequent .precipitation h.eat .treatments a.llow controlled r.elease o.f .these .constituents .either n.aturally (at .room .temperature) .or a.rtificially (at .higher t.emperatures). Most solution heat treatments often soften or anneal. And the alloys that are strengthened by SHT are called solution strengthened alloy. Elements in solid solution usually increase yield and tensile strength, other possibilities to increase strength is having finer grains. Solid s.olution i.s b.est .described a.s a h.omogeneous c.rystalline s.tructure i.n w.hich o.ne o.r more .types o.f a.toms o.r m.olecules m.ay .be p.artly substituted f.or t.he .original .atoms o.r .molecules .without c.hanging t.he .structure. T.his s.ubstitution has a. s.trengthening .effect o.n .the m.aterial. .Common s.trengthening .elements are c.hromium, .cobalt, .iron, m.olybdenum, .rhenium, t.antalum .and t.ungsten [7]. A.s .already mentioned .in c.hapter 1.3, s.olid-s.olution .strengthening .takes .place i.n γ .phase. T.he a.ddition .of f.or ..example m.olybdenum e.xpands .the l.attice .and .cobalt r.educes t.he l.attice .when .replacing i.ron .in .the s.uperalloy .matrix. A.n .expansion o.f t..he l.attice c.reates a.n i.nternal s.train. T.he e.xpansion .affects .the m.ismatch .with t.he s.trengthening p..recipitate .phase.

3**l.t h.as b.een s.hown t.hat t.he**

.stacking f.ault .energy .is r.educed i.n t.he p.resence o.f s.olid-s.olution s.trengtheners. .This .will .make .it ..more .difficult f.or .dislocations, t.hus c.ross-s.lip a.t .high t.emperatures .is r.estrained [8] [9]. Solid solution s.trengtheners

1**can also have a beneficial** i.nfluence **on the** c.orrosion **and oxidation resistance. Superalloys .with sufficiently large .chromium content will .form a protective** o.xide **film that** c.overs **the surface** [8]. **2.** 5.2 **Precipitation**

strengthening They are done in order to bring out the desirable strengthening precipitates and control other secondary phases. They include carbides, borides, TCP etc. The aging process increases hardness and strength but at the cost of reduction in ductility. As described in chapter 1.3, .gamma prime is f.ormed during a.ging by .the p.recipitation of

1aluminium and .titanium. The .slightly .different .lattice parameter of γ.' creates a s.mall misfit .important for .two reasons. First o.f all it g.uarantees a low γ/γ' surface energy which is e.ssential for a .stable m.icrostructure and i.mproves the p.roperties at e.levated temperatures. Secondly, a .negative m.isfit, i.e. γ' has a .smaller

l.attice p.arameter t.han

1γ, will .facilitate the f.ormation of r.afts and by .those m.eans .possibly .reduce the .creep rate.

The m.isfit is c.ontrolled by t.he .composition of t.he s.uperalloy, p.articularly by altering t.he .aluminium-titanium .ratio, but .also by t.he aging t.emperature [8] [10]. 2.6 MECHANISM OF AGING The s.trength of .metals is i.mproved by .restrict t.he m.otion of .dislocations .through t.he metals. .One .approach to a.chieving .this .improvement is t.o form a u.niform .distribution of .closely .spaced s.ub-micron .sized .particles t.hroughout an a.lloy. The .particles, .which restrict .the .dislocation m.otions in t.he .alloy are .known as .precipitate. Not .every a.lloy can be p.recipitation s.trengthened. The .particles are .formed by .precipitation, w.hich i.nvolves a .series of h.eat t.reatment .steps. The f.irst s.tep is .solution h.eat .treatment. This involves .heating the a.lloy up .to a .temperature t.hat r.esults in t.he .atoms of .the a.lloying element .being d.issolved w.ithin the s.olid .structure .formed by t.he .array of .atoms of t.he main .element. For .Al-Cu alloys, .the c.opper atoms dissolve .into .the a.rray of aluminum a.toms. The .dissolved s.tructure is t.hen r.etained at a.mbient .temperatures by cooling t.he a.lloy .rapidly, such .as by w.ater q.uenching. Figure. 9:

2Variation in hardness with aging temperature of laser deposited IN718

.After c.ooling, precipitates a.re f.ormed either .by n.atural a.ging o.r a.rtificial .aging. With .natural a.ging, .the p.recipitates f.orm .at r.oom t.emperature. W.ith a.rtificial .aging, t.he .precipitates f.orm .when a.n a.lloy .is .heated t.o a. t.emperature l.ower t.han t.he s.olution h.eat .treatment t.emperature. Only c.ertain .alloys w.ill .undergo n.atural .aging. The .other .alloys .must .be a.rtificially .aged. Regardless o.f t.he a.ging p.rocess, a.s t.he p.recipitation p.rocess .proceeds 0the .precipitates go .through a. s.eries o.f s.tages, .with .changes

3.in t.he .size, f.orm .and c.omposition o.f t.

he .precipitates. The .particular .stage

3o.f t.he .precipitates has .a d.irect i. nfluence o. n t.he

.strength .of .the a.lloy. For a.rtificially a.ged a.lloys, t.his .is controlled b.y .the .aging t.emperature a.nd .time. At a.ny .particular a.ging t.emperature, t.here i.s .an a.ging t.ime a.t .which .the a.lloy w.ill reach i.ts m.aximum s.trength. This .maximum s.trength c.orresponds to a. specific s.tage o.f .the f.orm a.nd .composition o.f t.he p.recipitates. Aging f.or a t.ime t.hat i.s t.oo .short .or t.oo .long will .result i.n l.ess t.han m.aximum a.lloy s.trength. For a.rtificially a.ged a.lloys, t.he .aging .temperature .affects t.he

m.aximum s.trength

3t.hat c.an b.e o. btained, a.nd t.

he t.ime required t.o r.each m.aximum s.trength. F.or .naturally a.ged a.lloys, t.he .strength i.ncreases .over t.ime. .The t.ime r.equired t.o r.each m.aximum .strength d.epends o.n .the .alloy. F.inally, .precipitation .strengthening c.an b.e .combined .with .cold-w.orking .to g.ive e.ven g.reater .alloy s.trength. 2.7 AGING EFFECT IN SUPERALLOYS 2.7

1.1 Contraction in superalloys Shrinkage d.uring use of s.uperalloys and the

fundamental m.echanisms have been discussed i.n s.everal studies [26] [27]. Marucco [27] m.easured lattice c.ontraction after aging at .intermediate t.emperatures between 450°C 600°C i.n 20Cr-25Ni steel, Sanicro 71 and I.nconel 690 w.hich a.mounted to 0.024, 0.040 and 0.038 % respectively. This study .also show that due to the aging there arose of a little ordered area in the alloys. Nath et al. have been i.nvolved in s.everal studies [27], to find out the a.ging

1effects on different .nickel-based .alloys, s.uch as .Nimonic 80A, a .wrought nickel-based precipitation- hardened

s.uperalloy u.sed as a b.olting m.aterial in s.team turbines. By u.se of

1.X-ray diffractometry t.hey proved .that the lattice p.arameter was .reduced d.ue to aging at 4.50- 600 °C and .the kinetics of .the .contraction was i.nvestigated. The m.aximum lattice .parameter .contraction was

o.btained d.uring aging .at 450°C f.or 30000 h a.nd m.easured

10.115 %. According to N.ath et al. the l.attice contraction w.as due to .short range o.rdering (SRO) and l.ong range .ordering (LRO) arisen d.uring aging. Electron d.iffraction studies .performed on N.imonic 80A c.orroborated the .existence of SRO b.ased on Ni2Cr .and the .transformation into

L.RO o.wing to l.ong-t.erm aging. The .lattice p.arameter .contraction depends o.n the .composition .of t.he .ordered p.hase. Marucco and Nath [27] have .measured .the lattice p.arameter c.ontraction in Ni2Cr a.nd Ni3Cr a.fter aging at .475°C.

1Ni3Cr exhibited a .small .contraction in .the n.eighbourhood of 0.05 % a.fter 10 000 h. The

l.attice p.arameter c.ontraction

1in Ni2Cr .under the s.ame conditions are .almost 5 times

l.arger. In p.revious w.ork c.arried out at b.y Nath, the l.attice c.ontraction in d.ifferent

1.nickel-based .superalloys and the .austenitic stainless s.teel X6CrNiTi18-10 .was m.easured. Cylindrical .specimens of the l.ength 100 mm .were a.ged at 450, 500 .and 550°C and the s.hrinkage .strain was

m.easured a.fter 300, 1000 and 3000 h.ours in a .c.oordinate measurement .machine. They .found that, it i.s

1obvious .that the contraction of .the a.lloys is s.ignificant .already after .300 h of

.aging and b.etween 3.00 h and 1.000 h the s.hrinkage

1.rate is .slowing down a.nd is .almost ..constant between 1.000 h and 3.000 h.

The .lattice .parameter of the .alloys was .measured b.efore and a.fter the a.ging w.ith X-ray .diffraction. 2.7

1.2 Short range ordering (SRO) and long range ordering (LRO) Short

r.ange o.rdering .arises in .all Ni-Cr alloys, i.rrespective of t.he p.resence o.f other a.lloy .elements. Small, o.rdered a.reas in .the s.ize of n.anometers a.re

1formed in an o.therwise .disordered .matrix. The .ordering .takes

p.lace w.hen a.toms of d.ifferent t.ypes are m.ore .attracted to e.ach other .than the .same type. The s.hort r.ange o.rdered

1.phase .forms at .stoichiometric .compositions, e.g. AB, A2B and A3B or at .off-stoichiometric .compositions .also but there is a

c.ondition of .lower kinetics. Ni2Cr is a o.rthorhombic o.rdering .phase that .occurs commonly in Ni s.uperalloys. The SRO f.ormation .takes p.lace d.uring either .cooling from s.olid-solution .temperature or at lower aging .temperature. The .degree of SRO d.ecreases with t.emperature,

1but it is .also .affected by the c.omposition. Studies on .ternary Ni-Cr-Fe a.lloys have s.hown that t.he enhancement of Ni c.ontent increases t.he .degree .of SRO and the .shortage of Fe c.ontent has

t.he o.pposite effect [26] [27]. Long time aging below a .critical temperature Tc will, for c.ertain a.lloy c.ompositions, result in .growth of SRO .nuclei, changes .short range .ordering p.hase i.nto long t.erm ordering .phase. Tc d.epends on t.he .composition of t.he alloy, b.ut is n.ormally .located .between 5.30°C and 580°C [27]. Even i.f long .range .ordered is n.on-existing a.bove Tc b.ut .short range o.rdered c.an e.xist at .temperatures a.bove T.c in s.toichiometric .alloys AxBy a.lloys w.hich .would be l.ong

1**range .ordered at .lower .temperatures,** S.ee **Figure** 10 **.for** example **Figure**

10 SRO represents by σ and LRO represents by S According t.o Rtishchev [28] .SRO and L.RO are .formed if .chromium c.ontent of .25-35 at% i.n .binary Ni-Cr .superalloy. In .commercial s.uperalloys, the f.ormation of L.RO is possible .only w.hen

1**.chromium content in γ .phase** a.fter **the γ'** p.recipitation .have **to .exceed 25%. The** .tendency **of**

N.i-Cr b.ased s.uperalloys to f.orm

1**LRO .can be** d.escribed **by the Z.- criterion** [28]. **Z is** c.alculated **on .the** a.tom **.content in γ, .after** p.recipitation **of γ'** a.nd **minor .phases,** a.ccording **to .Equation** 1: $Z = \frac{Ni}{Cr+W+Mo}$ ..... Equation 1.

According t.o Rtishchev, L.RO occurs at a.pproximate value of

1**Z<3.0. The Ni2Cr .superlattice .stability is .affected** b.y **the**

a.lloy e.lements.

1**It .has .been .shown that the .presence of .tungsten and .molybdenum** s.tabilizes **the** s.uperlattice **while** t.he **presence** o.f **.cobalt has .a**

n.egative e.ffect on

3**t.he s.** tability **of t.he** s.tructure. The **d.** egree **of**

.long range .ordering and .the .kinetics d.epend on t.he a.ging t.emperature and .the c.omposition. By .increasing t.he .aging t.emperature n.ucleation r.ate .decreases while t.he .grain .growth r.ate will .increase. The m.aximum k.inetics is .obtained f.or the composition .Ni2Cr. The l.arger d.eviation f.rom the s.toichiometry the s.lower k.inetics of LRO i.s obtained. The p.resence of t.ungsten

1**and .molybdenum will .have an accelerating** e.ffect **on .the .order** k.inetics. **On** t.he **other .hand, the** k.inetics **is** s..trongly **subdued**

b.y t.he p.resence of .c.obalt and i.ron.

> 1**Nath et al.** [27] **showed** t.hat **.the .kinetics of** l.attice **.contraction** .affected by **the**

a.ging time and a.pplied .strain. They c.oncluded the r.esults from .their l.attice c.ontraction measurements .for N.imonic 8.0A shows .that, the c.ontraction is d.ivided in .three s.tages. During t.he f.irst

> 1**500 h .the .contraction rate was** h.igh. **During** t.he **.next 15 000 h. it became .very** s.low **and** t.hen **it**

a.ccelerated a.gain at l.onger a.ging t.ime. 2.7

> 1**.3 Negative creep The .term negative** c.reep **is** .generally u.sed **for .the** s.uperposition **of** t.wo **.opposite processes.**

C.ommon p.lastic .creep p.rocess r.epresents the .positive c.omponent and .lattice contraction .process due to o.rdering represents t.he n.egative c.omponent. Superalloys show .the n.egative c.reep as a .contraction d.uring c.reep t.est or .as an i.ncrease in s.tress .during .relaxation t.est [26]. It .has been a.lso s.hown [26] that t.he o.rdering of N.i2Cr .in the .form SRO a.nd LRO a.risen .during a.ging

> 1**at 550°C .and .below is** r.esponsible **of** l..attice **contraction.** This .phenomenon **.leads to**

d.imensional i.nstability and negative .creep in N.imonic 80A a.nd the b.inary

> 1**.alloy Ni-20wt%Cr.** This w.as **also .confirmed that** t.he presence **of**

.the .precipitation o.f γ' had n.o effect on t.he process. CHAPTER 3 EXPERIMENTAL PROCEDURE 3.1 DIMENSION OF INCONEL TENSILE SPECIMEN 3.2 CHEMICAL COMPOSITION OF INCONEL 718

> 7**Table 1: chemical composition in weight percent Ni** Cr **Fe Nb Mo Ti Al**

53.5 19 18.5 4.5 3 1 0.5 3.3 AGING TREATMENT To study the aging effect of Inconel 718 three specimens are analyzed at different conditions. First one is studied at no aging condition or as received sample and other two are as heat treatment specimen HT1 and HT2 aged at different conditions. HT1 and HT2 first both solid solutionized at 955ºC for 1hr/AC and the aging conditions are given below in table 2: Table 2: Heat treatment process of HT1 and HT2 specimens HT1 ? ? ? 955ºC for 1hr; air cool to RT 718ºC for 8hr; furnace cool to 621ºC 621ºC for 18hr; air cool to RT HT2 ? ? 955ºC for 1hr; air cool to RT 718ºC for 8hr; air cool to RT 3.4 LIGHT OPTICAL MICROSCOPE Figure 11: Lieca optical microscope The metallographic analyses were carried out before and after the aging heat treatment. The samples were carefully polished on emery paper in decreasing order of coarseness successively using 100, 320, 900, 1200 and 1500 grit Sic paper. The grinded s.urface of the .specimens .was .polished on colloidal silica contained velvet polishing c.loth. To making visible the microstructure etching were done by using

waterless kalling solution containing

> 115 g CuCl2, 100 ml HCl and 100 ml ethanol on the

polished surfaces for 30 to 40 seconds. Microscopic e.xamination of .the .etched surface o.f s.pecimens w.as .successfully c.ompleted u.sing a .metallurgical .digital microscope (Lieca) .through .which .the .resulting m.icrostructure of t.he s.amples was a.ll photographically .recorded. For high resolution microstructures SEM and FESEM has also been used. 3.5 XRD Figure 12: X-ray diffraction machine In this technique we evaluate the precipitate phase present in the Inconel 718 such as γ, γ′, γ″ and δ. The XRD scanning was done in the range of 30º to 110º and t.he scanning rate was 1º per minute. After that the graph was a.nalyzed in X.-pert h.igh score s.oftware. 3.6 HARDNESS TEST EQUIPMENT For .hardness t.esting, the sample was grinded and polished and for heat treated sample oxide layer was removed. During this experiment 10 readings were taken at different positions from the sample. The parameters for the hardness test at which performed: load=10 kg and dwell time=10 sec. Figure 13: Vickers hardness testing machine. CHAPTER 4

> 9RESULTS AND DISCUSSION 4 .1 OPTICAL MICROSTRUCTURE OF AS

RECEIVED Figure 14:

> 9Optical microstructure of as received at

10x, 20x and 50x (fig.a,b,c) The microstructure is showing that the laser scan pattern is bidirectional as we discussed above. The fig.14c, shows the zig-zag pattern during the deposition primary dendrites grow at the angle of +45º and -45º. There is no precipitate phase present in the microstructure clearly shown. 4.2 OPTICAL MICROSTRUCTURE OF SINGLE STAGE AGING(HT2) Figure 15: Optical microstructure of single stage aging at 50x, 100x(a,b) Above fig.16 (a,b) showing there is no grain boundaries present in the microstructure. XRD shows some precipitate Fe0.64Ni0.36 and Cr.19Fe.70Ni.11 present in the matrix. 4.3 OPTICAL MICROSTRUCTURE OF TWO STAGE AGING(HT1) Figure 16: Optical microstructure of two stage at 10x, 20x, 50x and 100x(fig.a,b,c,d) Two stage aging images shown in fig.17 at different and lower magnification, they are showing dendritic growth. During aging for longer time the grain growth is possible because in hardness test showing less hardness then the single stage. 4.4 SEM MICROSTRUCTURE OF AS RECEIVED Figure 17:

> 8SEM images of as received at 100x and

500x(a,b) The fig.18 shows the

> 8SEM images of as received inconel 718

at lower magnification, because at higher magnification there was no phase or precipitate particles to shown. At lower magnification some particles are visible but confirmed unless done XRD of as received sample. 4.5 SEM MICROSTRUCTURE OF HT2 Figure 18: SEM images of single stage aging 1Kx, 2Kx, 5Kx, 20Kx(a,b,c,d) According to above fig.19 shows the precipitate forms in single stage aging and distributed uniformly in the matrix. These precipitates are responsible for the increase in hardness. 4.6 SEM MICROSTRUCTURE OF HT1 Figure 19: SEM images of two stage aging at 10Kx, 20Kx, 25Kx and

1Kx(a,b,c,d) The microstructure of two stage aging shown in fig.20, due to aging 26 hr the precipitate forms but precipitates grow and dissolve again in matrix. So we can hardly see some precipitates in the microstructure but XRD clarify that presents of precipitate. 4.7 PHASE ANALYSES Figure 20: Phases present in all specimens showing with symbols The XRD analyses showing the phases present in the as received, HT2 and HT1. The Fe0.64Ni0.36 is present in all the samples so we can consider it as matrix phase. At single stage aging Cr.19Fe.70Ni.11 precipitate forms which increase the hardness and strength, while in single stage aging there is present Mo1.24Ni0.76 (δ) phase which is orthorhombic crystal structure. This phase is softer and reduces in hardness. 4.8 VICKERS HARDNESS TEST Hardness 450 400 350 300 250 200 150 100 50 0 as received sample single stage(HT2) two stage(HT1) Figure 21: Hardness values of specimens in VHN According to above fig. 17, showing the average hardness of as received specimen as 260.2 VHN. After heat treatment of HT2 and HT1 show the hardness increases 397.8 VHN and 345 VHN respectively. Single stage aging(HT2) shows the increase in hardness by 34%, due to precipitate forms, while two stage aging(HT1) shows the less increase in hardness because of the formation of acicular phases. 4.9 TENSILE TEST RESULT Table 3: Results of tensile tests of age hardened samples compared with as-received sample of Inconel 718 specimens 0.2% Yield stress (proof stress) (MPa) Ultimate tensile stress (MPa) Fracture stress(MPa) As received 521.79 810 801 Single stage(HT2) 904.04 1083.75 1077.5 Two stage(HT1) 976.46 1125 1111.25 The breaking point of the specimens is at the middle, so results of the tensile tests are valid. Differences in the tensile properties are influence by the crystallographic texture and the distribution of the precipitates. As shown in table 2, two stage aging specimen get higher stress values then single stage aging, but relatively low plastic elongation. Figure 22: Stress-strain curves of as received, single stage and two stage aging specimens 4.10 CONCLUSIONS The optical microstructure shows the pattern of the laser processing is bidirectional. This In718 single crystal or directionally solidified is deposited on the polycrystalline stainless steel substrate. Directionally solidified component is very hard to deposit on the polycrystalline substrate. The SEM microstructure shows the presence of more precipitate in single stage then two stage aging. It means for longer time of aging some phases dissolve or show growth. XRD analyses confirm the presence of precipitates in the different aging conditions. Two stage aging shows the acicular phase, which arise after the long time aging and softer phase. With the aging time hardness increases but after a certain time period the hardness starts decreases. HT2 showing higher hardness then the HT1 because of the absence of the (δ) delta phase. Stress-strain curve in elastic region or modulus of elasticity changes after heat treatment. The strength of two stage aging sample is higher than the single stage but the reduction in ductility. This can be related by the phase formation after the heat treatment. 4.11 FUTURE SCOPE OF WORK No signs of corrosion were seen in the samples even after prolonged exposure to atmospheric conditions. This might be an indication of enhanced corrosion resistance. Corrosion studies should be carried out in order to get a deep inside for this property. High temperature tensile can be conducted after aging about 650º C to find out the changes in mechanical properties and microstructure. Inconel 718 generally used for high temperature applications such as gas turbine blades. At such high temperature applications creep is the dominant mode of failure so study creep behaviour should be carried out. REFERENCES [1] C.Slama and M.Abdellaoui, Structural characterization of the aged Inconel 718, Journal of Alloys and Compounds 306, 277-284, 2002. [2] W. Sims, C., Stoloff, N., Hagel, Superalloys II, October,19 ed. (Intersceince, Wiley, n.d.), pp. 615. [3] J. Davis: Heat Resistant Materials, Wiley-interscience, pp.589-591,1997. [4] J. Saarimäki: The Mechanical Properties of Lattice Truss Structures with Load- Bearing Shells Made of Selectively Laser Melted Hastelloy XTM, KTH, 2011. [5] R.C.Reed: The Superalloys (Cambridge University Press, Cambridge, UK, 2006),pp. 370-372, 2012 [6] M.Dehmas, J.Lacaze, A.Niang, and B.Viguier, TEM Study of high temperature precipitation of Delta phase in Inconel 718 alloy, Advances in Material Science and Engineering, 2011. [7] Davis, J.R.: Heat resistant Materials. Materials Park: ASM International,1997. [8] Sims, C.T., Stoloff, N.S., Hagel, W.C: superalloys II. New York: Wiley- interscience,1987. [9]. Donachie, M.J., Donachie, S.J.: Superalloys. A Technical Guide. 2nd edition. Materials Park: ASM International.2002. [10]. Orakzai, K.: Effect of Carbon Content on the Properties of CMSX-4. Finspång: Siemens Industrial Turbomachinery AB, 2004. [11] G.P. Dinda, A.K. Dasgupta and J. Mazumder: Texture control during laser deposition of nickel-based superalloy, Scripta Materialia,vol.67,pp.503–506, 2012. [12] C.-M. Kuo, Y.T. Yang, H.Y. Bor, C.-N.Wei, C.-C. Tai:Aging effects

on the microstructure and creep behavior of Inconel 718 superalloy, Materials Science and Engineering,pp.289–294,2009. [13] I.Tabernero, A.Lamikiz, S.Martı´nez: Evaluation of the mechanical properties of Inconel 718 components built by laser cladding, International Journal of Machine Tools & Manufacture,pp. 465–470,2011. [14] Xiaoming Zhao, Jing Chen, Xin Lin: Study on microstructure and mechanical properties of laser rapid forming Inconel 718, Material science and engineering,vol.478,pp.119-124,2008. [15] J. J. Valencia, T. McCabe, K. Hensl, J. 0. Hansenz, and A. Bose: Microstructure and mechanical properties of inconel 625 and 718 alloys processed by powder injection molding, The Minerals, Metals &Materials Society,PP.936-944,1994. [16] W. D. Cao: Superalloys 7 18. 625 and Various Derivatives, edited by E. Loria,pp 147-160,1991 [17] Bi GJ, Gasser A, Wissenbach K, Drenker A, Poprawe R: Investigation on the direct laser metallic powder deposition process via temperature measurement,Appl. Surf. Sci,pp.253-261,2006. [18] Liu JC, Li LJ: In-time motion adjustment in laser cladding manufacturing process for improving dimensional accuracy and surface finish of the formed part, Opt. Laser Technol,vol.36(6),pp.477–83,2004. [19] Lewis GK, Schlienger E.: Practical considerations and capabilities for laser assisted direct metal deposition, Mater. Des. ,vol.21(4),pp.417–23,2000. [20] Wu X, Mei J.: Near net shape manufacturing of components using direct laser fabrication technology, J. Mater. Process Technol,vol.13(2-3),pp.266–70,2003. [21] C.P. Paul, P. Ganesh, S.K. Mishra, P. Bhargava, J. Negi, A.K. Nath: Investigating laser rapid manufacturing for Inconel-718 components, Optics and Laser Technology,pp. 800–805,2007. [22] X. Zhao, J. Chen, X. Lin, W. Huang: Study on microstructure and mechanical properties of laser rapid forming Inconel 718, Materials Science and Engineering,pp.119– 124,2008. [23] D. Clarka, M.R. Bacheb, M.T. Whittakerb: Shaped metal deposition of a nickel alloy for aero engine applications, Journal of Materials Processing Technology,pp.439– 448,2008. [24] D. Dudzinski, A. Devillez, A. Moufki, D. Larrouquere, V. Zerrouki, J. Vigneau: A review of developments towards dry and high speed machining of Inconel 718 alloy, International Journal of Machine Tools and Manufacture ,vol.44,pp. 439–456,2004. [25] F. Liu, X. Lin, G. Yang, M. Song, J. Chen, W. Huang: Microstructure and residual stress of laser rapid formed Inconel 718 nickel-base superalloy, Optics and Laser Technology,vol.43,pp. 208–213,2011. [26] Moverare, J.: Shrinkage and ageing of Ni-base alloys at intermediate temperatures (400-600C),pp.358-367,2005. [27] Marucco, A., Nath, B.: Effects of ordering on the properties of Ni-Cr alloys. J.Mat. Sci., 23, pp.2107-2114,1988. [28] Rtishchev, V.V.: Structure transformations and property changes of Ni- base superalloys on ageing. Mat. Adv. Power Enf.,(1), pp.889-898,1994